

# Short-distance QCD corrections to $K^0\bar{K}^0$ mixing at next-to-leading order in Left-Right models

VÉRONIQUE BERNARD<sup>a</sup>, SÉBASTIEN DESCOTES-GENON<sup>b</sup>, LUIZ VALE SILVA<sup>a,b</sup>

(a) *Groupe de Physique Théorique, Institut de Physique Nucléaire, UMR 8606,  
CNRS, Univ. Paris-Sud, Université Paris-Saclay, 91405 Orsay Cedex, France*

(b) *Laboratoire de Physique Théorique, UMR 8627,  
CNRS, Univ. Paris-Sud, Université Paris-Saclay, 91405 Orsay Cedex, France*

## Abstract

Left-Right (LR) models are extensions of the Standard Model where left-right symmetry is restored at high energies, and which are strongly constrained by kaon mixing described in the framework of the  $|\Delta S| = 2$  effective Hamiltonian. We consider the short-distance QCD corrections to this Hamiltonian both in the Standard Model (SM) and in LR models. The leading logarithms occurring in these short-distance corrections can be resummed within a rigorous Effective Field Theory (EFT) approach integrating out heavy degrees of freedom progressively, or using an approximate simpler method of regions identifying the ranges of loop momentum generating large logarithms in the relevant two-loop diagrams. We compare the two approaches in the SM at next-to-leading order, finding a very good agreement when one scale dominates the problem, but only a fair agreement in the presence of a large logarithm at leading order. We compute the short-distance QCD corrections for LR models at next-to-leading order using the method of regions, and we compare the results with the EFT approach for the  $WW'$  box with two charm quarks (together with additional diagrams forming a gauge-invariant combination), where a large logarithm occurs already at leading order. We conclude by providing next-to-leading-order estimates for  $cc$ ,  $ct$  and  $tt$  boxes in LR models.

A natural extension of the Standard Model (SM) is provided by Left-Right (LR) symmetric models, which explain the left-handed structure of the SM through the existence of a larger gauge group  $SU_C(3) \times SU_L(2) \times SU_R(2) \times U_Y(1)$ , broken first at a scale  $\mu_R$  of the order of the TeV (inducing a difference between left and right sectors) followed by an electroweak symmetry breaking occurring at a scale  $\mu_W$  [1–5]. This extension induces the presence of heavy spin-1  $W'$  and  $Z'$  bosons predominantly coupling to right-handed fermions, introducing a new CKM-like matrix for right-handed quarks, as well as charged and neutral heavy Higgs bosons with an interesting pattern of flavour-changing currents [6, 7]. Such a framework has been revived in the recent years for its potential collider implications when parity restoration in the LHC energy reach is considered [8, 9].

Many different mechanisms can be invoked to trigger the breakdown of the left-right symmetry. Historically, LR models were first considered with doublets in order to break the left-right symmetry spontaneously. Later the focus was set on triplet models, due to their ability to generate both Dirac and Majorana masses for neutrinos and thus introducing a see-saw mechanism [10, 11]. LR models provide also interesting candidates for a  $Z'$  boson as currently hinted at by  $b \rightarrow s\ell\ell$  observables [12–14]. Stringent constraints come from electroweak precision observables [15] and from direct searches at LHC [16, 17], pushing the limit for LR models to several TeV. Studies in the framework of flavour physics suggest also that the structure for the right-handed CKM-like matrix should be quite different from the left-handed one, far from the manifest or pseudo-manifest scenarios [18–22].

In this setting, a particularly important indirect constraint comes from kaon-meson mixing, favouring a mass scale for the new scalar particles of a few TeV or beyond [23–27]. This comes from the very accurate measurement of kaon mixing together with the possibility of generating kaon mixing in the LR model by exchanging at tree level a heavy neutral Higgs boson with flavour-changing neutral couplings. As usual in flavour physics, such a process involves dynamics occurring at several different scales: the heavy degrees of freedom  $W'$  of mass of order  $\mathcal{O}(\mu_R)$ , the degrees of freedom occurring at the electroweak symmetry breaking  $\mu_W$ , and the dynamics at low energies (around the charm quark mass or below). The first range is addressed directly in the LR model whereas the last energy domain is tackled by lattice QCD computations, which now provide accurate kaon mixing matrix elements for the operators in the SM and beyond [28]. The two domains can be bridged thanks to the effective Hamiltonian approach, which also provides an elegant framework to take into account higher-order QCD corrections [29].

Indeed, short-distance QCD corrections prove to have an important impact on the computation of kaon mixing in the Standard Model, easily increasing or decreasing the contributions from the different diagrams to the amplitude by 50%. This large impact stems from the multi-scale nature of the problem, leading to the presence of large logarithms (for instance  $\alpha_s \cdot \log(m_c^2/M_W^2)$ ). This requires a resummation of the leading logarithms, which can be obtained by applying an Effective Field Theory (EFT) approach to the problem. One considers a tower of effective Hamiltonians where heavy degrees of freedom are integrated out progressively and which can be matched onto each other. The renormalisation group equations provide the resummation of the large logarithms in a natural way, which requires dedicated computations of two-loop diagrams [30–36].

In the early days of these computations, an alternative method was proposed in Refs. [37, 38], attempting at catching the main effects of large logarithms by considering the relevant regions of momentum integration in the diagrams. This method of regions was applied to resum the leading logarithms both in the SM [38] and LR models [39, 40], with a much more limited amount of computation, since most of the method relies on anomalous dimensions already known.

The aim of the present paper is to reconsider the evaluation of short-distance QCD corrections needed to evaluate neutral-meson mixing (and in particular kaon meson mixing) precisely in the case of LR models. In Sec. 1, we recall a few elements of the two methods in the SM case at Leading Order (LO), before illustrating how the method of regions of Refs. [38–40] could be extended to Next-to-Leading Order (NLO) and comparing the results with the EFT case. In Sec. 2, we discuss the additional contributions arising in LR models and we compute short-distance QCD corrections

at NLO using the method of regions. In Sec. 3, we compare our results with the EFT approach in the case of the  $cc$  box with  $W$  and  $W'$  exchanges (together with additional diagrams to get a gauge-invariant contributions), where a large logarithm occurs already at leading order, and we discuss also the case of  $ct$  and  $tt$  boxes. We provide our conclusions in Sec. 4. Several appendices are devoted to more technical aspects of the computation.

# 1 Short-distance QCD corrections in the Standard Model

## 1.1 EFT computation

The analysis of kaon mixing is customarily performed in the framework of the effective Hamiltonian, separating short and long distances in the following way [29]

$$H = \frac{G_F^2}{4\pi^2} M_W^2 \left[ \lambda_c^{LL} \lambda_c^{LL} \eta_{cc} S^{LL}(x_c) + \lambda_t^{LL} \lambda_t^{LL} \eta_{tt} S^{LL}(x_t) + 2 \lambda_t^{LL} \lambda_c^{LL} \eta_{ct} S^{LL}(x_c, x_t) \right] b(\mu_h) Q_V + h.c., \quad (1)$$

where the local  $|\Delta S| = 2$  operator involved is

$$Q_V = (\bar{s}^\alpha \gamma_\mu P_L d^\alpha)(\bar{s}^\beta \gamma^\mu P_L d^\beta) = \frac{1}{4} (\bar{s}d)_{V-A} (\bar{s}d)_{V-A}. \quad (2)$$

This result involves the short-distance QCD corrections  $\eta_{cc}, \eta_{tt}, \eta_{ct}$  (note that in the literature these corrections are also called  $\eta_1, \eta_2, \eta_3$ , respectively).  $S^{LL}$  are related to the usual Inami-Lim functions depending on the quark masses through  $x_i = m_i^2/M_W^2$  (see Eq. (113)) and  $\lambda_i^{LL} = V_{id}^{CKM} (V_{is}^{CKM})^*$  combines two CKM matrix elements. The derivation of this result relies on the GIM mechanism to eliminate the  $\lambda_u^{LL}$  terms.

The matrix element  $\langle \bar{K}^0 | H | K^0 \rangle$  can be computed knowing  $\langle \bar{K}^0 | Q_V | K \rangle$  from lattice QCD simulations at a low hadronic scale  $\mu_h$  of a few GeV [28] and  $b(\mu_h)$  is a function which combines with  $\langle \bar{K}^0 | H | K^0 \rangle$  to form a renormalisation-group invariant quantity. This function contains the scale dependence of the Wilson coefficient due to its running down to the hadronic scale. Note that in the literature this function is sometimes absorbed into the definition of the QCD correction factor:

$$\bar{\eta} = \eta b(\mu_h), \quad (3)$$

which is thus scale and renormalisation-scheme dependent. In the discussion of LR models we will deal with the scale-dependent  $\bar{\eta}$  factors, as it proves easier to deal with the latter in the case of several  $|\Delta S| = 2$  local operators mixing among each other. In the absence of the resummation of short-distance QCD corrections we would have  $\eta_{ct} = \eta_{cc} = \eta_{tt} = 1$ . This clearly also holds for the scale-dependent terms  $\bar{\eta}$ .

For completeness, we summarise a few important features for the determination of the short-distance corrections  $\eta$  at the order of leading and next-to-leading logarithms. In the case of the  $tt$  box [31], the Wilson coefficient can be obtained easily by integrating out both the  $W$  boson and the  $t$  quark at a high scale  $\mu_{tW} = \mathcal{O}(m_t, M_W)$ . The corresponding effective Hamiltonian consists of a single operator  $Q_V$  multiplied by a Wilson coefficient obtained by matching at  $\mu_{tW}$ . The coefficient is then run down to  $\mu_h$ .

The  $cc$  box [33, 41] has the additional complication that the charm quark cannot be integrated out at the same time as the  $W$  boson. One first integrates out the  $W$  boson, leading to a  $|\Delta S| = 1$  effective Hamiltonian of the form

$$H_c = \frac{4G_F}{\sqrt{2}} \sum_{U,V=u,c} (V_{Us}^{CKM})^* V_{Vd}^{CKM} (C_+ O_+^{UV} + C_- O_-^{UV}), \quad (4)$$

involving the  $|\Delta S| = 1$  operators

$$O_{\pm}^{UV} = \frac{O_1^{UV} \pm O_2^{UV}}{2}, \quad (5)$$

with

$$O_1^{UV} = \frac{1}{4}(\bar{s}^\alpha U^\alpha)_{V-A}(\bar{V}^\beta d^\beta)_{V-A}, \quad O_2^{UV} = \frac{1}{4}(\bar{s}^\alpha U^\beta)_{V-A}(\bar{V}^\beta d^\alpha)_{V-A}, \quad (6)$$

where  $\alpha, \beta$  are colour indices.  $|\Delta S| = 2$  transitions occur through bilocal operators of the form  $\int d^4y T[H_c(x)H_c(y)]$  yielding a sum of four bilocal operators  $O_{ij}$  (with  $i, j = \pm$ ):

$$H_{\text{eff}}^{|\Delta S|=2}(cc) = \frac{4G_F^2}{2} \lambda_c^2 \sum_{i,j=\pm} C_i C_j O_{ij}, \quad (7)$$

$$O_{ij}(x) = \frac{-i}{2} \int d^4y T[O_i^{cc}(x)O_j^{cc}(y) + O_i^{uu}(x)O_j^{uu}(y) - O_i^{cu}(x)O_j^{uc}(y) - O_i^{uc}(x)O_j^{cu}(y)] \quad (8)$$

The Wilson coefficients of the operators  $O_{ij}$  (equal to the product  $C_i C_j$ ) must be evolved from  $\mu_W = \mathcal{O}(M_W)$  down to  $\mu_c$ , before matching onto a theory without charm containing the single operator  $Q_V$ , see Eq. (2) (at NLO, the matching must be performed at  $\mathcal{O}(\alpha_s)$ ). The resulting coefficient must be evolved down to  $\mu_h$ . Note that in principle one would have to add a set of penguin operators in Eq. (4) (for more detail see Refs. [32, 35]).

Finally, the top-charm contribution  $\eta_{ct}$  requires a more involved analysis of the renormalisation group structure of the theory [35]. The first step consists in integrating out the  $t$  and  $W$  quarks, adding to the  $|\Delta S| = 1$  Hamiltonian Eq. (4) a set of penguin operators. The resulting expression is

$$H_{\text{eff}}^{|\Delta S|=2}(ct) = \frac{4G_F^2}{2} \lambda_c \lambda_t \left[ \sum_{i=\pm, j=1, \dots, 6} C_i C_j O_{ij} + C_7 Q_7 \right], \quad (9)$$

$$O_{ij}(x) = -\frac{i}{2} \int d^4y T[2O_i^{uu}(x)O_j^{uu}(y) - O_i^{cu}(x)O_j^{uc}(y) - O_i^{uc}(x)O_j^{cu}(y)], \quad j = 1, 2, \quad (10)$$

with a similar result for bilocal operators involving penguins  $j = 3, \dots, 6$ , and an additional  $|\Delta S| = 2$  operator

$$Q_7 = \frac{m_c^2}{g^2 \mu^{2\epsilon}} \frac{1}{4}(\bar{s}d)_{V-A}(\bar{s}d)_{V-A}, \quad (11)$$

which is required as the bilocal operators  $O_{ij}$  exhibit an ultraviolet divergence which has to be regularised by a local counterterm (this problem does not occur for the  $cc$  box as the divergences cancel due to the GIM mechanism). This results into the logarithmic contribution  $-x_c \log x_c$  to the corresponding Inami-Lim function contained in  $S^{LL}(x_c, x_t)$ , not present in the  $cc$  case. This means that there is a mixing between the bilocal operators  $O_{ij}$  and the local operator  $(\bar{s}d)_{V-A}(\bar{s}d)_{V-A}$  at leading order, even before taking QCD corrections into account. This undesirable feature can be avoided by introducing the  $1/g^2$  normalisation factor for  $Q_7$ , so that this mixing is treated on the same footing as QCD radiative corrections and a common RGE framework can be applied to discuss the mixing of all the operators [29, 30]. This theory can be evolved down to the charm quark mass, where it is matched onto a theory without charm, containing the single operator  $Q_V$  once again, to be evolved down to  $\mu_h$ . Neglecting any effects of the five-flavour theory allows one to write a relatively simple expression for  $\eta_{ct}$  [35]. Note that in this expression the penguin operators have been switched off since their contribution has been found to be of the order of 1%.

Finally, we should notice that the initial conditions of the Wilson coefficients are determined by integrating out the top quark and the  $W$  boson simultaneously, thus neglecting the evolution between the scales  $\mu_t$  and  $\mu_W$  (a detailed discussion of this issue can be found in Ref. [35]).

## 1.2 Method of regions at leading order

Historically, the first determination of  $K^0\bar{K}^0$  mixing in the SM did not take into account the short-distance QCD corrections [42, 43]. A method to determine these corrections by resumming the leading logarithms was then developed in the case of the charm quark [37], the inclusion of the top quark being studied in Ref. [38]. It was further used to calculate the mixing in Left-Right symmetric models [39, 40]. In the following this method will be called “method of regions” (MR) for reasons that will become clear soon.

Contrarily to more recent works which use the EFT approach presented in Sec. 1.1, this method aims at catching the main features in an approximate way. Let us summarise briefly the underlying idea, basically amounting to resum the leading logarithms with the help of renormalisation group equations. We consider first the calculation of the  $\mathcal{O}(\alpha_s)$  corrections to the one-loop  $c$  quarks contribution to the Green function with the insertion of four weak currents ( $cc$  box). This was done in Refs. [31, 33], taking into account the GIM mechanism and leading to

$$\langle H^c(\mu_h) \rangle = \langle H^c(\mu_h) \rangle^{(0)} + \frac{\alpha_s(\mu_h)}{4\pi} \langle H^c(\mu_h) \rangle^{(1)} + \mathcal{O}(\alpha_s^2), \quad (12)$$

with

$$\begin{aligned} \langle H^c(\mu_h) \rangle^{(0)} &= \frac{G_F^2}{4\pi^2} \lambda_c^2 m_c^2(\mu_h) \langle Q_V(\mu_h) \rangle^{(0)}, \\ \langle H^c(\mu_h) \rangle^{(1)} &= \frac{3G_F^2}{2\pi^2} \lambda_c^2 m_c^2(\mu_h) \langle Q_V(\mu_h) \rangle^{(0)} \left[ -C_F \log\left(\frac{m_c^2}{\mu_h^2}\right) \right. \\ &\quad \left. + \frac{N-1}{2N} \left( 2 \log\left(\frac{m_c^2}{M_W^2}\right) - \log\left(\frac{m_c^2}{\mu_h^2}\right) \right) \right] + \dots \end{aligned} \quad (13)$$

where  $N$  denotes the number of colours and the ellipsis contains constant terms proportional to  $\langle Q_V(\mu_h) \rangle^{(0)}$  and contributions from unphysical operators that are not relevant here. Indeed, in the leading-logarithm approximation one only keeps track of the logarithms in Eq. (13) and resums them to all orders in perturbation theory.

Instead of performing the whole calculation, Vysotskiĭ rather proposed in Ref. [38] to analyse the dressing of the box diagrams with gluons in all possible ways. The one-loop momentum  $k$  of the original graph is kept fixed, and one has to identify the region for the gluon momentum  $q$  leading to a logarithmic behaviour. These logarithms are then resummed at fixed  $k$  and finally the integration over  $k$  is performed. Let us illustrate this procedure in the case of the  $\alpha_s \cdot \log(m_c^2/M_W^2)$  contribution in Eq. (13).

Vysotskiĭ showed that the integration over  $q^2$  in the range  $[k^2, M_W^2]$  in the left diagram in Fig. 1 leads to a term  $\log(k^2/M_W^2)$ , responsible for the second logarithm (for  $k^2 = \mathcal{O}(m_c^2)$ ) in Eq. (13). Cutting this graph along the two internal quark lines yields the set of multiplicatively renormalised operators contributing to each half of the diagram, giving rise to the bilocal operators  $O_{ij}$  introduced in Eq. (8). The employ of RGE over the relevant range of momentum for  $q^2$  provides the resummation of logarithms as required

$$\frac{1}{2} \left( \frac{\alpha_s(k^2)}{\alpha_s(M_W^2)} \right)^{8/\beta_0} - \left( \frac{\alpha_s(k^2)}{\alpha_s(M_W^2)} \right)^{2/\beta_0} + \frac{3}{2} \left( \frac{\alpha_s(k^2)}{\alpha_s(M_W^2)} \right)^{-4/\beta_0} = \sum_{i,j=+,-} t_{ij} \left( \frac{\alpha_s(k^2)}{\alpha_s(M_W^2)} \right)^{d_{ij}}, \quad (14)$$

where the exponents  $d_{ij} = \gamma_{ij}^{(0)} / (2\beta_0)$  come from the anomalous dimensions  $\gamma_{ij}$  of the bilocal operators  $O_{ij}$  involved (corresponding to the sum of the anomalous dimensions for the individual  $|\Delta S| = 1$  operators),  $\beta_0 = (11N - 2f)/3$  is the first term in the expansion of the usual renormalisation group function that governs the evolution of the QCD coupling constant (with  $f$  the number of active flavours), and

$$t_{ij} = \frac{1}{4} (1 + i + j + N) \delta_{ij}, \quad i, j = \pm, \quad (15)$$

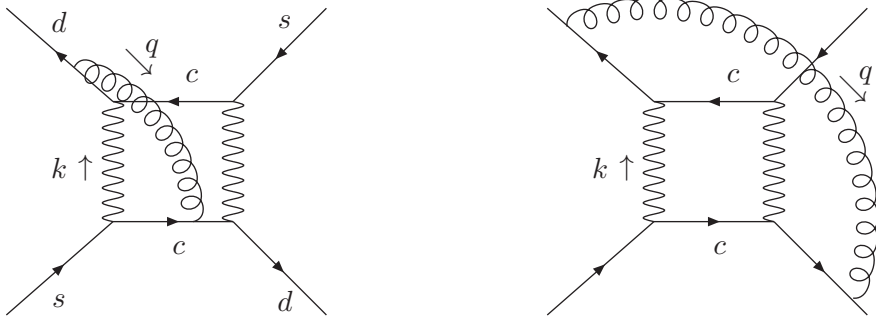


Figure 1: Typical SM  $cc$  box diagram leading to the contributions  $\log(m_c^2/M_W^2)$  (four possibilities for gluon exchanges in total, left) and  $\log(m_c^2/\mu_h^2)$  (two possibilities in total, right) in the computation of short-distance QCD corrections to kaon mixing.

is a factor arising from the matching of the bilocal operators  $O_{ij}$  onto the  $|\Delta S| = 2$  local operator, leading to the same integral but with different coefficients due to the different projectors involved.

After having introduced the resummation of large logarithms coming from the operator evolution, we still have to perform the remaining integration over the momentum  $k$ , typically

$$\int d^4k f(k^2) \left( \frac{\alpha_s(k^2)}{\alpha_s(M_W^2)} \right)^\gamma, \quad (16)$$

( $\gamma = 0$  corresponds to the original loop integral without radiative corrections), which is treated in two different ways depending on the behaviour of the one-loop integral. If it has a power law behaviour dominated by a single mass scale  $m$  i.e. ( $a \neq 0$ )

$$\int d^4k f(k^2) \sim (m^2)^a, \quad (17)$$

we can replace the integral as follows

$$\int d^4k f(k^2) \left( \frac{\alpha_s(k^2)}{\alpha_s(\mu^2)} \right)^\gamma \sim (m^2)^a \left( \frac{\alpha_s(m^2)}{\alpha_s(\mu^2)} \right)^\gamma. \quad (18)$$

This is our case in Eq. (13) since  $\langle H^c(\mu_W) \rangle^{(0)} \propto m_c^2$ , and we obtain a sum of contributions to the Wilson coefficient of the form

$$m_c^2 \left( \frac{\alpha_s(m_c^2)}{\alpha_s(M_W^2)} \right)^{d_{ij}}. \quad (19)$$

If we expand it at leading order in  $\alpha_s \log(m_c^2/M_W^2)$  using the evolution of  $\alpha_s$  between two scales

$$\alpha_s(m_1) = \frac{\alpha_s(m_2)}{1 - \beta_0 \frac{\alpha_s(m_2)}{2\pi} \log \left( \frac{m_2}{m_1} \right)}, \quad (20)$$

we obtain

$$\frac{\alpha_s}{4\pi} \log \left( \frac{m_c^2}{M_W^2} \right) \sum_{i,j=+,-} \frac{\gamma_{ij}^{(0)}}{2} t_{ij}, \quad \sum_{i,j=+,-} \frac{\gamma_{ij}^{(0)}}{2} t_{ij} = 12 \frac{N-1}{2N}, \quad (21)$$

showing that the resummed expression Eq. (19) indeed reproduces the large logarithm in Eq. (13).

The resummations leading to the two other logarithms in Eq. (13) is performed in a similar way. The last logarithm comes from a diagram where the gluon is attached to two external quarks of same flavour, see the right diagram in Fig. 1. The relevant range of integration of  $q^2$  is  $[\mu_h^2, k^2]$ , where  $\mu_h$  is the low hadronic scale. The relevant anomalous dimension is then the one attached to the  $|\Delta S| = 2$  local operator. Once again, the remaining integration over  $k^2$  can be simplified by noticing that only

the scale  $k^2 = \mathcal{O}(m_c^2)$  is relevant (for more detail, see Refs. [38, 39]). Finally, the first logarithm in Eq. (13) comes from the evolution of the charm quark mass from the  $m_c$  scale down to  $\mu_h$ . In the SM, taking into account the GIM mechanism, all the box diagrams with internal quark lines of the same flavour exhibit such a power law behaviour for which this procedure holds.

In the case of the top-charm box, matters are a bit more complicated. Indeed the corresponding original integral has not a simple power law behaviour, but instead a logarithmic behaviour as stated before, i.e.  $\int_{m_1^2}^{m_2^2} dk^2 f(k^2) = \log(m_2^2/m_1^2)$ . In this case one defines the LO averaging weight  $R(\gamma, m_1, m_2)$  such that

$$(\log(m_2^2/m_1^2))^{-1} \int_{m_1^2}^{m_2^2} \frac{dk^2}{k^2} \left( \frac{\alpha_s(k^2)}{\alpha_s(\mu^2)} \right)^\gamma = R(\gamma, m_1, m_2) \left( \frac{\alpha_s(m_1^2)}{\alpha_s(\mu^2)} \right)^\gamma. \quad (22)$$

The method of regions amounts thus to computing the Wilson coefficients at the lower scale  $m_1^2$  and to multiply them by the appropriate factors  $R$ .

One should in principle also consider contributions coming from the graphs where one or both  $W$  bosons are replaced by Goldstone bosons. Actually, the sum of those diagrams ( $WW$ ,  $WG$ ,  $GG$ ) is independent of the gauge chosen for the electroweak bosons, and the discussion can be performed in the unitarity gauge where only the  $WW$  diagram should be considered.

An additional comment is in order concerning the anomalous dimensions and the number of active flavours. In the EFT approach one performs a matching onto an effective Hamiltonian valid between two scales determined by the number of flavours involved, integrating out a quark flavour each time the scale gets lower than the corresponding quark threshold. One then runs the Wilson coefficient from one scale to the other. In Vysotskii's original procedure, it is assumed that the  $t$  and  $b$  quarks do not appear in large logarithms so that  $f$  could be chosen as 3 or 4, arguing that the difference between the numerical values of  $\beta_0$  (involved in the running of the operators) for  $f = 5$  and  $f = 4$  would anyway be very small [38]. Thus only two scales have to be considered,  $\mu_c$  and the low scale  $\mu_h$  at which the matrix element of the relevant operator is computed. In a similar vein, in the case of the presence of the logarithm in  $\langle H^c(\mu_h) \rangle^{(0)}$ . Vysotskii did not distinguish the anomalous dimension of the  $|\Delta S| = 2$  local operator between the scale  $\mu_c$  and  $\mu_W$  and below  $\mu_c$ .

In Ref. [39], the same method was reexpressed in a slightly different language. Expressed in the SM case, it amounts to considering the bilocal operators Eqs. (8) and (10), running them from the high scale  $\mu_W$  to a scale  $k^2$ , and multiplying the evolution factors given by the RGE with the evolution factor coming from the local  $|\Delta S| = 2$  operator from the scale  $k^2$  down to  $\mu_h$ . This provides the two contributions to large logarithms from the diagrams displayed in Fig. 1. The integration with respect to  $k^2$  is then performed by the procedure outlined in Eqs. (18) and (22).

The LO values of the short-distance QCD corrections in the SM for the kaon system using this method are given in Tab. 1 and compared with the values obtained from a systematic EFT approach [35]. We included the flavour thresholds neglected by Vysotskii. The numerical results are obtained using the same inputs as in Ref. [35], namely  $m_t(m_t) = 167$  GeV,  $m_c(m_c) = \mu_c = 1.3$  GeV,  $M_W = 80$  GeV,  $\Lambda^{(4)} = 0.310$  GeV. The matchings onto the effective theories are performed at  $\mu_b = 4.8$  GeV, whereas the high scale  $\mu_W$  is chosen differently depending on the box considered:  $\mu_W = 130$  GeV when a  $t$  quark is involved in order to take care of the fact that in the EFT approach the top quark and the  $W$  boson are integrated out at the same time (hence  $\mu_W$  is an average of the two masses), whereas  $\mu_W = M_W$  when only  $c$  and  $u$  quarks are involved and only the  $W$  boson has to be integrated out in the diagram. As can be seen in Tab. 1, the method of regions works very well at leading order.

### 1.3 Method of regions at next-to-leading order

We will now extend the method of regions to determine the short-range corrections  $\eta$  at NLO taking advantage that the anomalous dimensions of all the operators involved have been determined for

	$\eta_{tt}$	$\eta_{ct}$
MR	$0.598 + 0.028 = 0.626$	$0.345 - 0.011 = 0.334$
EFT	$0.612 - 0.038 = 0.574$	$0.368 + 0.099 = 0.467$

Table 1: *Comparison of the SM short-distance QCD corrections using the method of regions (MR) and a systematic EFT approach. The first number corresponds to the LO (resummation of  $(\alpha_s \log(m_c/\mu))^n$ ) and the second to the NLO (resummation of  $\alpha_s(\alpha_s \log(m_c/\mu))^n$ ). Note that in the case of  $\eta_{ct}$  the LO in the four-quark theory corresponds to a resummation of  $(\alpha_s \log(m_c/M_W))^n \log(m_c/M_W)$  and the NLO to  $(\alpha_s \log(m_c/M_W))^n$ . Flavour thresholds are taken into account. Both approaches lead to an identical result in the case of  $\eta_{cc}$ , not shown here.*

the SM and LR models [36].<sup>1</sup> Following closely what is done in the EFT approach one uses the renormalisation group equations for the Wilson coefficients to determine them at  $\mathcal{O}(\alpha_s)$  (requiring to know both matching and anomalous dimensions at this order). Second one should calculate the  $\mathcal{O}(\alpha_s)$  corrections to the operators involved. Indeed considering both kinds of corrections are mandatory in order to get a scheme-independent result.

We can check that extending the method of regions at NLO is appropriate by applying it to the SM case first. We use the result of Ref. [33] for the calculation of the  $\mathcal{O}(\alpha_s)$  corrections of the  $|\Delta S| = 2$  local operator  $Q_V$  appearing in the effective four- and three-quark theories for the computation of  $\eta_{cc}$ . The expressions of  $\eta_{tt}$  and  $\eta_{ct}$  at NLO are given in App. A and are obtained by including the same diagrams and integration ranges as in the LO case, but considering the additional  $\mathcal{O}(\alpha_s)$  corrections for the matching and evolution and modifying the averaging procedure to take them into account. The numerical results are gathered in Tab. 1.

We do not provide  $\eta_{cc}$  using the MR as it turns out to be identical to the one obtained in the EFT approach, see Eq. (XII.31) in Ref. [29] for example. Let us just stress the importance of the  $\mathcal{O}(\alpha_s)$  corrections  $\beta_{ij}$ , ( $i, j = \pm$ ) coming from the matching of the product of operators  $O_{\pm}$  onto the  $|\Delta S| = 2$  local operators. We obtain, using the same input as before except by setting  $\mu_W = M_W$ :

$$\eta_{cc} = 0.89 + (0.62 - 0.19) \quad (\text{EFT}), \quad (23)$$

where the first number corresponds to the LO result (in Ref. [29], the LO result corresponds to a calculation with the LO value of  $\alpha_s$  leading to  $\eta_{cc} = 0.74$ ), the second and third numbers are the NLO contributions, the former coming from  $\beta_{ij}$  and the latter corresponding to the remaining contributions. The matching at  $\mu_W$  is also important: neglecting the scheme-invariant quantity  $\alpha_s(\mu_W)(B_i + B_j - J_{ij})$  (where  $B_{\pm}$  comes from the matching of the SM to  $O_{\pm}$  operators at  $\mu_W$  and  $J$  comes from the anomalous dimension matrix of these operators) would lead to a 7% increase coming almost entirely from the  $B_i$  terms.

In Tab. 1 the NLO contributions obtained with the method of regions are compared to the EFT approach. The agreement is quite good for the short-distance corrections with two same quarks in the loop, which do not involve any large logarithm in the calculation without QCD corrections. A somewhat larger 10% discrepancy is obtained in the case of  $\eta_{tt}$  which can be traced back to the fact that the top quark is not integrated out at the same time as the  $W$  boson contrary to the EFT case. The MR method is much less accurate at NLO for  $\eta_{ct}$ , where large logarithms are present: our way of extending Vysotskiĭ's method yields a result with a 30% error.

Note that  $\eta_{cc}$  and  $\eta_{ct}$  have been calculated at NNLO in the EFT approach leading to a significant positive shift for  $\eta_{cc} = 1.87(76)$  [41] and a 7% increase for  $\eta_{ct} = 0.496(47)$  [44]. This illustrates the importance of higher orders in the evaluation of the short-distance QCD corrections.

<sup>1</sup>Some additional anomalous dimensions will be needed for the EFT approach, as will be shown in Sec. 3.

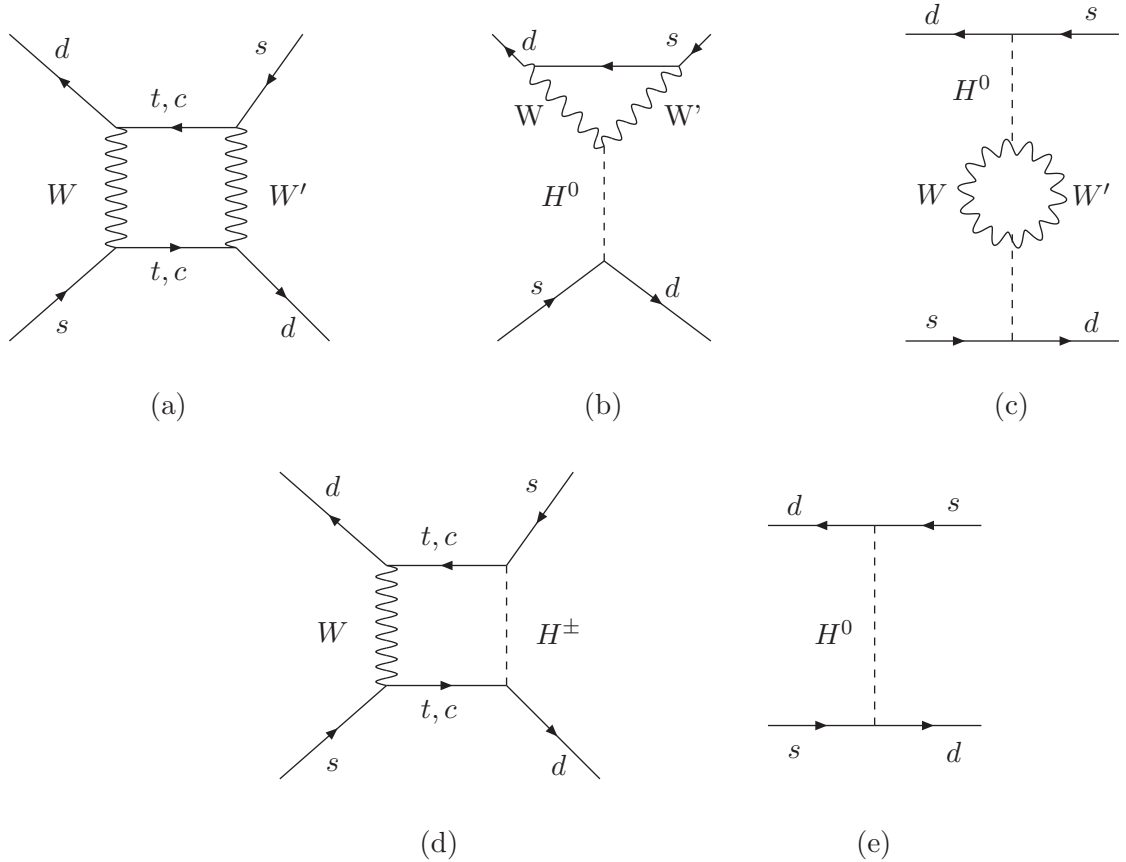


Figure 2: *Diagrams for kaon mixing in Left-Right models: the sum of the first row (a)+(b)+(c) is gauge invariant, whereas the second row is also corresponds to additional diagrams of interest. We do not show the diagrams where one or several gauge bosons are replaced by the corresponding Goldstone bosons. Diagrams with  $u$ -quarks in the loop are suppressed by powers of  $m_u$  and are thus not considered.*

## 2 QCD corrections for Left-Right models

### 2.1 Contributions to kaon mixing in Left-Right models

The LR models generate corrections for kaon mixing compared to the SM case. We will exploit the hierarchy between the left-right and electroweak symmetry breaking scales, reflected by the hierarchy of masses between  $W$  and  $W'$  bosons (as well as heavy Higgs bosons), and we keep only the first correction in  $\beta = (M_W/M_{W'})^2$  (and assuming  $\omega = (M_{W'}/M_H)^2 = \mathcal{O}(1)$ ).

The problem differs from the SM on several points due to the different structure of  $W'$  couplings. First, the GIM mechanism cannot be invoked since the two different CKM-like matrices are involved (one for left-handed quarks, the other one for right-handed quarks). Second, the effective theory at the low scale involves two different  $|\Delta S| = 2$  operators which are not multiplicatively renormalised. Third, the  $WW'$  box together with the contributions from Goldstone bosons is not gauge invariant (in contrast with the SM case), which means that additional diagrams involving heavy neutral Higgs exchanges together with a  $W$  and a  $W'$  must be considered [45–47], shown in the first row of Fig. 2. Additional diagrams are given in the second row of the same figure.

We will give the results for the method of regions in the t'Hooft-Feynman gauge for the electroweak gauge bosons (we will use the unitary gauge later, when we compute corrections in the EFT framework). The contributions from the gauge bosons and their associated Goldstone bosons at the

scale  $\mu_W$ , diagram 2(a), are given by Refs. [7, 39, 45, 46, 48]

$$\begin{aligned} \langle A^{(\text{box})} \rangle &= \frac{G_F^2 M_W^2}{4\pi^2} 2\beta h^2 \langle Q_2^{LR} \rangle \\ &\times \sum_{UV=c,t} \lambda_U^{LR} \lambda_V^{RL} \sqrt{x_U x_V} [(4 + x_U x_V \beta) I_1(x_U, x_V, \beta) - (1 + \beta) I_2(x_U, x_V, \beta)], \end{aligned} \quad (24)$$

where the  $|\Delta S| = 2$  scalar operator  $Q_2^{LR} = (\bar{s}^\alpha P_L d^\alpha)(\bar{s}^\beta P_R d^\beta)$  appears. The quark masses enter as  $x_i = (m_i/M_W)^2$ , and are evaluated at the scale  $m_i$  for heavy quarks, and at the scale  $\mu_h$  for the strange quark (we set  $m_u = m_d = 0$ ).  $\lambda_i^{PQ} = (V_{id}^P)^* V_{is}^Q$  collects the product of CKM-like matrices, the couplings from  $SU(2)_L$  and  $SU(2)_R$  gauge groups appear through  $h = g_R/g_L$ , and  $I_1$  and  $I_2$  are modified Inami-Lim functions which can be expanded at leading order in  $\beta$ :

$$I_1 = \frac{x_U \log x_U}{(1 - x_U)(x_U - x_V)} + (U \leftrightarrow V) + \mathcal{O}(\beta), \quad I_2 = \frac{x_U^2 \log x_U}{(1 - x_U)(x_U - x_V)} + (U \leftrightarrow V) - \log \beta + \mathcal{O}(\beta). \quad (25)$$

In the t'Hooft-Feynman gauge, one can identify the various contributions to Eq. (24) coming from  $WW'$  (term proportional to  $I_1(x_U, x_V, \beta)$ ),  $GG'$  (term  $\propto x_U x_V \beta \cdot I_1(x_U, x_V, \beta)$ , of higher order in  $\beta$ ),  $GW'$  (term  $\propto I_2(x_U, x_V, \beta)$ ) and  $WG'$  (term  $\propto \beta \cdot I_2(x_U, x_V, \beta)$ , of higher order).

We rewrite the transition amplitude Eq. (24) in a different form and keep the leading term in  $x_c$ :

$$\begin{aligned} \langle A^{(\text{box})} \rangle &= \frac{G_F^2 M_W^2}{4\pi^2} 2\beta h^2 \langle Q_2^{LR} \rangle \\ &\times \left( \lambda_c^{LR} \lambda_c^{RL} S^{(\text{box})}(x_c) + \lambda_t^{LR} \lambda_t^{RL} S^{(\text{box})}(x_t) + (\lambda_c^{LR} \lambda_t^{RL} + \lambda_t^{LR} \lambda_c^{RL}) S^{(\text{box})}(x_c, x_t) \right), \end{aligned} \quad (26)$$

at one-loop order in the absence of QCD corrections and at leading order in  $\beta$ , with

$$S^{(\text{box})}(x_c, x_t) = \sqrt{x_c x_t} \left[ \frac{x_t - 4}{x_t - 1} \log(x_t) + \log(\beta) \right] + \beta \cdot \mathcal{O}(\beta, x_c^{3/2}), \quad (27)$$

$$S^{(\text{box})}(x_t) = x_t \left( \frac{x_t^2 - 2x_t + 4}{(x_t - 1)^2} \log(x_t) + \frac{x_t - 4}{x_t - 1} + \log(\beta) \right) + \mathcal{O}(\beta^2), \quad (28)$$

$$S^{(\text{box})}(x_c) = x_c (4 \log(x_c) + 4 + \log(\beta)) + \beta \cdot \mathcal{O}(\beta, x_c^2). \quad (29)$$

We notice that a large  $\log(x_c)$  arises for the  $cc$  box, whereas  $ct$  and  $tt$  boxes are dominated by the single scale  $m_t$ . The extra  $\log(\beta)$  present in these equations comes from the  $I_2$  function which is due to boxes with one Goldstone boson  $G$  exchanged in the t'Hooft-Feynman gauge.

The contributions from the vertex correction 2(b) and self-energy diagrams 2(c) read

$$\begin{aligned} \langle A^{(\text{vert})} \rangle &= -2\beta \omega h^2 \frac{G_F^2 M_W^2}{4\pi^2} \langle Q_2^{LR} \rangle S_V(\beta, \omega) \sum_{U,V=c,t} \lambda_U^{LR} \lambda_V^{RL} \sqrt{x_U x_V}, \\ \langle A^{(\text{self})} \rangle &= -32\beta \omega h^2 \frac{G_F^2 M_W^2}{4\pi^2} \langle Q_2^{LR} \rangle S_S(\beta, \omega) \sum_{U,V=c,t} \lambda_U^{LR} \lambda_V^{RL} \sqrt{x_U x_V}, \end{aligned} \quad (30)$$

with the two functions [27, 46, 47]

$$S_V(\beta, \omega) = \left[ \frac{\omega^2 + 1}{\omega} [I_a(0) - I_a(M_H^2)] + \left( \frac{\omega - 1}{\omega} \right)^2 \frac{M_W^2}{\beta} I_b(M_H^2) \right] + \mathcal{O}(\beta), \quad (31)$$

$$S_S(\beta, \omega) = [I_a(0) - I_a(M_H^2)] + \mathcal{O}(\beta). \quad (32)$$

We only kept the leading power of  $\beta$  in the above expressions, so that for  $m_i, M_W \ll M_{W'}$  and an arbitrary  $M_{W'}/M_H$

$$I_a(0) - I_a(M_H^2) \simeq -1 + (1 - \omega) \log \left| \frac{1 - \omega}{\omega} \right| + \mathcal{O}(\beta), \quad (33)$$

$$I_b(M_H^2) \simeq \frac{\beta}{M_W^2} \left[ \omega + \omega^2 \log \left| \frac{1 - \omega}{\omega} \right| \right] + \mathcal{O}(\beta^2). \quad (34)$$

As can be seen no logarithms in  $\beta$  are generated by these diagrams.

Another contribution must be considered, the one represented in Fig. 2(e). In these models, heavy neutral Higgs bosons can exhibit flavour-changing neutral couplings generating  $|\Delta S| = 2$  transitions at tree level. The corresponding transition has the form

$$\langle A^{(H^0)} \rangle = -\frac{4G_F}{\sqrt{2}} u \beta \omega \langle Q_2^{LR} \rangle \sum_{i,j=c,t} \lambda_i^{LR} \lambda_j^{RL} \sqrt{x_i(\mu_H) x_j(\mu_H)}, \quad (35)$$

with  $u = (1 + r^2)^2 / (1 - r^2)^2$  and  $r = |\kappa_1 / \kappa_2|$  the ratio of Higgs vacuum expectation values triggering electroweak symmetry breaking.

Finally, we have contributions coming from the box with a  $W$  boson and a heavy charged Higgs (of a mass similar to the neutral Higgs boson considered above), Fig. 2 (c):

$$\langle A^{(H^\pm \text{ box})} \rangle = \frac{G_F^2 M_W^2}{4\pi^2} \langle Q_2^{LR} \rangle \sum_{U,V=c,t} \lambda_U^{LR} \lambda_V^{RL} S_{LR}^H(x_U, x_V, \beta\omega), \quad (36)$$

with

$$S_{LR}^H(x_U, x_V, \beta\omega) = 2\omega\beta u \sqrt{x_U x_V} [x_U x_V I_1(x_U, x_V, \beta\omega) - I_2(x_U, x_V, \beta\omega)], \quad (37)$$

the first term coming from boxes with a Goldstone boson (relevant only for  $tt$  boxes) and the second term from boxes with a  $W$  boson.

In the above expressions, we assumed that the breakdown of the left-right symmetry is triggered only by non-vanishing vacuum expectation values of scalar fields charged under  $SU(2)_R$  (the structure remains similar, but the prefactor is modified in the case of non-vanishing VEV for scalar fields charged under  $SU(2)_L$  [49]).

## 2.2 Method of regions

Short-distance QCD corrections, denoted  $\eta_{UV}$ , will correct the previous expressions. We are now in a position to compute these corrections at NLO since the anomalous dimensions needed for the calculation have been determined in Ref. [36] and are summarised in App. B for completeness.

Ref. [39] considered the LO case, which can be obtained following the same steps as described in Sec. 1.2, with the following modifications: the bilocal operators involve one left-handed and one right-handed  $|\Delta S| = 1$  operators ( $O_l^{VLL}$  and  $O_r^{VRR}$ ), which are matched onto the LR model at different scales ( $\mu_W$  versus  $\mu_R$ ), and the matching has to be performed onto two  $|\Delta S| = 2$  local operators rather than a single one. Note that in Ref. [39] the two additional diagrams involving heavy neutral Higgs exchanges together with a  $W$  and a  $W'$  bosons, diagrams 2(b) and 2(c), have been neglected arguing that in the t'Hooft-Feynman gauge their contributions are small for large enough neutral Higgs masses.

One can adapt Ref. [39] to include the NLO contributions and derive the expression for  $\bar{\eta}_{UV}$  within the method of regions without flavour thresholds (it is rather trivial to take these thresholds into account, but the expressions are somewhat lengthy). One gets in this case

$$\begin{aligned} \langle A^{(\text{box})} \rangle &= \frac{G_F^2 M_W^2}{4\pi^2} 2\beta h^2 \sum_{a=1,2} \langle Q_a^{LR} \rangle \\ &\times \sum_{UV=c,t} \lambda_U^{LR} \lambda_V^{RL} \sqrt{x_U x_V} [4\bar{\eta}_{a,UV}^{(W'1)} I_1(x_U, x_V, \beta) - \bar{\eta}_{a,UV}^{(W'2)} I_2(x_U, x_V, \beta)], \end{aligned} \quad (38)$$

with the two  $|\Delta S| = 2$  local operators

$$Q_1^{LR} = (\bar{s}^\alpha \gamma_\mu P_L d^\alpha)(\bar{s}^\beta \gamma^\mu P_R d^\beta), \quad Q_2^{LR} = (\bar{s}^\alpha P_L d^\alpha)(\bar{s}^\beta P_R d^\beta). \quad (39)$$

In order to express the short-distance QCD correction  $\bar{\eta}_{a,UV}^{(W'1)}$  ( $U$  and  $V$  denote the quarks in the loop with  $m_U \leq m_V$ ), we start by defining

$$\xi_{a,UV}^{(W'1)} = \sum_{r,l=\pm,i=1,2} \left( \frac{\alpha_s(m_V)}{\alpha_s(\mu_h)} \right)^{-d_l - d_r + d_i + d_m} \left( \frac{\alpha_s(m_U)}{\alpha_s(\mu_h)} \right)^{-d_m} \left( \frac{\alpha_s(\mu_W)}{\alpha_s(\mu_h)} \right)^{d_l} \left( \frac{\alpha_s(\mu_R)}{\alpha_s(\mu_h)} \right)^{d_r} \times \left[ \left( 1 + \frac{\alpha_s(\mu_h)}{4\pi} \hat{K} \right) \hat{W} \right]_{ai} \times R^{NLO} \left( -d_l - d_r + d_i + 2d_m, \right.$$

$$\left. \left[ \hat{W}^{-1} \left( 1 - \frac{\alpha_s(\mu_W)}{4\pi} [J_l - B_l] - \frac{\alpha_s(\mu_R)}{4\pi} [J_r - B_r] + \frac{\alpha_s(m_U) + \alpha_s(m_V)}{4\pi} J_m \right) \left( \begin{array}{c} \tau_1^{rl} \\ \tau_2^{rl} \end{array} \right) \right]_i, m_V, \mu_W \right), \quad (41)$$

with  $d_{l,r}$  determined from the anomalous dimensions of the  $|\Delta S| = 1$  current-current operators,  $d_i$  from the corresponding  $|\Delta S| = 2$  local operator,  $d_m$  from the evolution of the masses,  $J_{l,r,i,m}$  the corresponding terms from the anomalous dimension matrix at NLO,  $\hat{W}$  being a diagonalisation matrix, and finally the values of the Wilson coefficients coming from the matching between the bilocal operators  $O_{rl}$  and the local  $|\Delta S| = 2$  operators are

$$\tau_1^{rl} = \tau_{rl}/4, \quad \tau_2^{rl} = 1/4, \quad \tau_{rl} = -(r + l + Nrl)/2. \quad (42)$$

For  $\bar{\eta}_{a,ct}^{(W'1)}$  and  $\bar{\eta}_{a,tt}^{(W'1)}$ , there are no large logarithms in the contribution from  $I_1$  in Eq. (27)-(28), the integral is dominated by  $k^2 = \mathcal{O}(m_V^2)$  and we have

$$\bar{\eta}_{a,ct}^{(W'1)} = \xi_{a,ct}^{(W'1)} [R^{NLO} \rightarrow R_1^{NLO}], \quad \bar{\eta}_{a,tt}^{(W'1)} = \xi_{a,tt}^{(W'1)} [R^{NLO} \rightarrow R_1^{NLO}] \quad (43)$$

where  $R^{NLO}$  should be replaced by  $R_1^{NLO}$  defined in Eq. (119).

$\bar{\eta}_{cc}^{(W'1)}$  should in principle be obtained by taking  $\xi_{a,ct}^{(W'1)}$  and replacing  $R^{NLO}$  by  $R_{\log}^{NLO}$  given in Eq. (117). However, the expression Eq. (41) resums the  $\alpha_s \log(m_c/M_W)^n \log(m_c/M_W)$  terms (counted as LO), plus some of the terms as  $(\alpha_s \log(m_c/M_W))^n$  (counted as NLO). Since  $I_1 = \log x_c + 1 + \mathcal{O}(x_c)$  provides contributions both at LO ( $\log x_c$ , with an average  $R_{\log}^{NLO}$ ) and NLO (1, with an average  $R_1^{NLO}$ ), we should separate the two contributions. This procedure<sup>2</sup> yields the modified expression

$$\bar{\eta}_{a,cc}^{(W'1)} = \frac{1}{1 + \log x_c} \left( \xi_{a,cc}^{(W'1)} \log(x_c) + \sum_{r,l=\pm,i=1,2} \left( \frac{\alpha_s(m_c)}{\alpha_s(\mu_h)} \right)^{-d_l - d_r + d_i} \times \left( \frac{\alpha_s(\mu_W)}{\alpha_s(\mu_h)} \right)^{d_l} \left( \frac{\alpha_s(\mu_R)}{\alpha_s(\mu_h)} \right)^{d_r} \hat{W}_{ai} \left[ \hat{W}^{-1} \left( \begin{array}{c} \tau_1^{rl} \\ \tau_2^{rl} \end{array} \right) \right]_i \right). \quad (44)$$

Similar expressions are obtained for the other short-distance QCD corrections given above, which

---

<sup>2</sup>A similar separation can be performed in the SM case for  $\eta_{ct}$ , as explained in App. A.

	$\bar{\eta}_{tt}$	$\bar{\eta}_{ct}$	$\bar{\eta}_{cc}$
$(W'1)$	$4.68 + 0.96 = 5.64$	$2.43 + 0.26 = 2.69$	$1.55 + 0.16 - 0.31 = 1.40$
$(W'2)$	$4.70 + 0.98 = 5.68$	$2.44 + 0.27 = 2.71$	$1.31 - 0.02 = 1.29$
$(H^0)$ , (vert), (self)	$4.66 + 0.98 = 5.64$	$2.42 + 0.27 = 2.69$	$1.26 + 0.02 = 1.28$
$(H1)$	$4.66 + 0.99 = 5.65$	-	-
$(H2)$	$4.66 + 0.97 = 5.63$	$2.42 + 0.27 = 2.69$	$1.31 - 0.02 = 1.29$

Table 2: *Short-distance QCD corrections at NLO for the LR contributions to kaon mixing with the method of regions. Flavour thresholds are taken into account. The  $\bar{\eta}$  are calculated at the hadronisation scale  $\mu_h = 1$  GeV with the parameters given in the text. The first (second) number corresponds to the LO (NLO, respectively) result.  $\alpha_s$  is always evaluated up to NLO. In the case of  $\bar{\eta}_{cc}$  the next-to-leading order is split into the NLO corrections to  $\log(x_c)$  (second number) and the NLO contribution to the non-logarithmic piece (third number). We do not indicate the value for (H1) when it corresponds to a higher order term in  $x_c$  in the effective Hamiltonian.*

are gathered in App. C. They collect the short-distance QCD corrections  $\bar{\eta}_{UV}$  for the other diagrams:

$$\langle A^{(H^0)} \rangle = -\frac{4G_F}{\sqrt{2}} u \beta \omega \sum_{a=1,2} \langle Q_a^{LR} \rangle \sum_{UV=c,t} \bar{\eta}_{a,UV}^{(H)} \lambda_U^{LR} \lambda_V^{RL} \sqrt{x_U x_V}, \quad (45)$$

$$\langle A^{(\text{vert})} \rangle = -2\beta\omega h^2 \frac{G_F^2 M_W^2}{4\pi^2} \sum_{a=1,2} \langle Q_a^{LR} \rangle \sum_{UV=c,t} \bar{\eta}_{a,UV}^{(H)} \lambda_U^{LR} \lambda_V^{RL} \sqrt{x_U x_V} S_V(\beta, \omega), \quad (46)$$

$$\langle A^{(\text{self})} \rangle = -32\beta\omega h^2 \frac{G_F^2 M_W^2}{4\pi^2} \sum_{a=1,2} \langle Q_a^{LR} \rangle \sum_{UV=c,t} \bar{\eta}_{a,UV}^{(H)} \lambda_U^{LR} \lambda_V^{RL} \sqrt{x_U x_V} S_S(\beta, \omega), \quad (47)$$

$$\begin{aligned} \langle A^{(H^\pm \text{ box})} \rangle &= \frac{G_F^2 M_W^2}{4\pi^2} \sum_{a=1,2} \langle Q_a^{LR} \rangle \\ &\times \sum_{U,V=c,t} \lambda_U^{LR} \lambda_V^{RL} \times 2\beta\omega u \sqrt{x_U x_V} [\bar{\eta}_{a,UV}^{(H1)} x_U x_V I_1(x_U, x_V, \beta\omega) - \bar{\eta}_{a,UV}^{(H2)} I_2(x_U, x_V, \beta\omega)], \end{aligned} \quad (48)$$

where we followed Ref. [39] to attribute the same scaling to the three contributions related to neutral Higgs exchanges (the momenta relevant for the method of regions are smaller than the high scales  $M_{W,W',H}$ ).

The results for  $\bar{\eta}_{2,UV} \equiv \bar{\eta}_{UV}$  are shown in Tab. 2 with the following inputs:  $m_t(m_t) = \mu_t = 170$  GeV,  $m_c(m_c) = \mu_c = 1.3$  GeV,  $\mu_b = 4.8$  GeV,  $M_W = \mu_W = 80.385$  GeV,  $M_{W'} = 1$  TeV,  $M_H \simeq 3$  TeV and  $\Lambda^{(4)} = 0.325$  GeV. They include the flavour thresholds. The LO results are in fairly good agreement with the calculation of Ref. [27]. The short-distance corrections  $\bar{\eta}_{1,UV}$  are at least an order of magnitude smaller than  $\bar{\eta}_{2,UV}$  and will not be considered further, in agreement with Refs. [26, 27].

Two contributions  $(W'2)$  and  $(H2)$  contain  $\log \beta$ , which can be considered either large or small depending on the hierarchy of the gauge bosons. In Tab. 2 and in App. C, we provide the expressions without resumming this logarithm. One may however be worried that for significant hierarchies between the left and right gauge sectors, a resummation would be needed also for  $\log \beta$ . Treating it in a similar way to  $\log x_c$ , we obtain the results gathered in Tab. 3, indicating a 10%-20% variation compared to the previous case for  $tt$  (and a smaller variation for  $ct$ ). We also show the mild dependence of the result on  $M_H$ .

	$\bar{\eta}_{tt}$	$\bar{\eta}_{ct}$
$(W'2)$	$4.86 + 7.32 - 5.26 = 6.92$	$2.52 + 1.91 - 1.51 = 2.92$
$(WH), \omega = 0.1$	$4.86 + 4.11 - 2.65 = 6.33$	$2.53 + 1.17 - 0.86 = 2.83$
$(WH), \omega = 0.8$	$4.84 + 6.70 - 4.76 = 6.79$	$2.52 + 1.77 - 1.40 = 2.89$

Table 3: *Same results as in Tab. 2, assuming that  $\log(\beta)$  is large and has to be resummed through  $R_{\log}$ . Note that in this case  $(WH)$  is sensitive to the value of  $\omega$ .*

### 3 NLO computation of $\bar{\eta}_{cc}^{LR}$ in the EFT approach

In Section 1, we have shown that the method of regions gives results in good agreement with those obtained using EFT in the SM ( $cc$  and  $tt$  boxes), when we start from diagrams exhibiting no large logarithms at leading order. The agreement is less satisfying in the case of the  $ct$  box where a large logarithm occurs. Moving to the LR models, one may thus worry that the  $WW'$  box with two charm quarks (exhibiting large  $\log(x_c)$  contributions) might not be computed accurately within the MR. We will thus determine the corrections also in the EFT framework. In this setting, it is more natural to discuss the short-distance QCD corrections to the gauge-invariant sum of the diagrams 2 (a), (b) and (c) involving two  $c$  quarks:

$$\langle A_{cc}^{LR} \rangle = \frac{G_F^2 M_W^2}{4\pi^2} 2\beta h^2 \langle Q_2^{LR} \rangle (\lambda_c^{LR})^2 4x_c S^{LR}(x_c, \beta, \omega), \quad (49)$$

with

$$S^{LR}(x_c, \beta, \omega) = 1 + \log(x_c) + \frac{1}{4} \log(\beta) + \frac{1}{4} F(\omega), \quad (50)$$

and

$$F(\omega) = 18\omega - (1 + 16\omega - 17\omega^2) \log|(1 - \omega)/\omega| \quad (51)$$

and we will calculate  $\bar{\eta}_{cc}^{(LR)}$  within the EFT approach, following the cases of the  $cc$  [33] and  $ct$  boxes [35] in the SM. Since we have also computed the short-distance QCD corrections for the LR model using the method of regions in Section 2 we will be able to compare both results.

As can be seen from Eq. (50), we have again a contribution  $\log \beta$  which can be treated either as a large logarithm or not. In our EFT computation, we will consider that this is not a large logarithm and that there is no need to resum this contribution. In addition to simplifying the computation, this assumption can be justified by the fact that  $\log \beta$  provides a subleading contribution numerically to Eq. (50) compared to  $\log x_c$ . Moreover, in the (admittedly different) context of the MR, there is almost no numerical difference between the values of  $\bar{\eta}_{ct}^{(LR)}$  and  $\bar{\eta}_{tt}^{(LR)}$  obtained resumming  $\log \beta$  or not.

The EFT computation will allow us to determine the mixing between the  $|\Delta S| = 1$  and  $|\Delta S| = 2$  operators in the four-quark theory, as well as the  $\mathcal{O}(\alpha_s)$  contributions to the  $|\Delta S| = 2$  operator in the effective four- and three-quark theories. In fact the latter contributions appear at NNLO thus beyond the order at which we work, but they will provide an estimate of the size of the NNLO terms. The comparison between the two methods and the consideration of higher orders (NNLO contributions, variation of the scales) will provide an estimate of the remaining uncertainties that we will discuss at the end of our evaluation. This piece of information will be used also to discuss the short-distance QCD corrections for the LR for the two  $ct$  and  $tt$  boxes.

### 3.1 Effective four-quark theory

Separating the short- and long-distance physics at a scale between  $\mu_c$  and  $\mu_W$  yields the following effective Hamiltonian

$$H = 8G_F^2 \beta h^2 \sum_{i,j=+,-} C_{ij}(\mu) O_{ij}(\mu) + C_{1,ij}(\mu) Q_1(\mu) + C_{2,ij}(\mu) Q_2(\mu) + \dots \quad (52)$$

where the two last terms on the right-hand side are required to absorb one-loop divergences. The local dimension-eight  $|\Delta S| = 2$  operators  $Q_a$  are defined as

$$Q_1 = \frac{m_c^2}{g^2 \mu^{2\epsilon}} (\bar{s} \gamma_\mu P_L d)(\bar{s} \gamma^\mu P_R d), \quad Q_2 = \frac{m_c^2}{g^2 \mu^{2\epsilon}} (\bar{s} P_L d)(\bar{s} P_R d). \quad (53)$$

According to the usual convention [29, 35], two inverse powers of the strong coupling constant have been introduced compared to  $Q_{1,2}^{LR}$  in order to avoid mixing already at the leading order. The coefficients  $C_{a,ij}$  are given by

$$C_{a,ij}(\mu) = C_{ij}(\mu) C_a^{\text{inf}}/\epsilon + C_a^r(\mu), \quad (54)$$

where  $C_a^r(\mu_W)$  can be determined from a matching at the scale  $\mu_W$  and  $C_a^{\text{inf}}$  is such that it cancels the divergence from the evaluation of the one-loop diagram Fig. 3 (see Eq. (59) below). Note that the running of  $C_a^r(\mu)$  is different from the one of  $C_{ij}(\mu)$ .

We consider here the complete set of diagrams necessary for gauge invariance shown in Fig. 2 (a), (b), (c). For the MR computation performed in Sec. 2.2, we computed a short-distance QCD factor for each relevant diagram ( $WW'$ ,  $GW'$ , vertex and self-energy): in this case, the 't Hooft-Feynman gauge is preferred to the unitarity gauge as it avoids divergences in individual diagrams [50]. In the EFT calculation, we consider the sum of all diagrams and we can work directly in the unitary gauge so that it is clear that Goldstone bosons do not contribute. Thus we will determine the NLO contribution of the operator  $\langle O_{ij}(\mu) \rangle$  which corresponds to one insertion of  $\gamma_\mu P_L \otimes \gamma^\mu P_L$  and one of  $\gamma_\nu P_R \otimes \gamma^\nu P_R$ . Following Ref. [33], we will work in the  $\overline{MS}$  scheme, with an anticommuting  $\gamma_5$  (NDR scheme) in  $D = 4 - 2\epsilon$  dimensions, and we use an arbitrary QCD  $R_\xi$  gauge. We keep non-vanishing strange and down quark masses to regularise infrared singularities (this regularisation leads to the appearance of unphysical operators which however do not affect the outcome of the computation [33]).

The ellipsis in Eq. (52) includes additional physical operators, such as  $|\Delta S| = 1$  local operators and the contribution of  $|\Delta S| = 1$  penguin operators, as well as the so-called evanescent operators. We do not write explicitly the  $|\Delta S| = 1$  local operators, but it should be noticed that their inclusion at one loop requires also to consider loop diagrams with QCD counterterms, canceling the divergences arising then. In the following we will neglect the contributions from penguin operators, which were shown to give either a small or vanishing contribution in the SM [32, 35]. On the other hand, we will consider the required evanescent operators, which play an important role for the evaluation of  $\eta_{cc}$ , as discussed in particular in Refs. [34, 51, 52].

#### 3.1.1 Evanescent operators

Evanescent operators appear in the discussion of the RGE evolution of the effective Hamiltonian. These operators occur in the definition of the Dirac algebra in  $D$  dimensions: they vanish for  $D = 4$  dimensions, but they appear as counterterms to physical operators multiplied by  $1/\epsilon$ . In principle, at each order of perturbation theory, new sets of evanescent operators are required, arising in the computation of radiative corrections to the physical and evanescent operators already present in the theory. In the context of the RGE for the effective Hamiltonian, the evanescent operators play a role

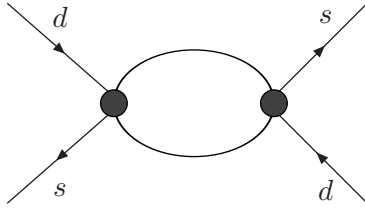


Figure 3: Diagram  $D_0$  in the effective four-flavour theory. Black circles denote the insertions of  $|\Delta S| = 1$  current-current operators.

in two different issues: first, the matrix elements of evanescent operators can affect the matching equation allowing one to determine the Wilson coefficients in the effective theory [51], and second, the presence of evanescent operators in counterterms for physical operators (and the other way around) means that both set of operators may mix under renormalisation [52]. In Refs. [51, 52], it was shown that a finite renormalisation of the evanescent operators could make their matrix elements vanish and that evanescent operators could not mix into physical ones at the level of the anomalous dimension matrix  $\gamma$ , so that evanescent operators do not contribute to the Wilson coefficients through matching or evolution. On the other hand, the renormalisation matrix  $Z$  of evanescent operators do contribute to the computation of the anomalous dimension matrix  $\gamma$  for physical operators, and thus must be taken into account to renormalise the effective theory and to determine its running.

In our case, we will need the following evanescent operators  $E_i[O]$  when we consider QCD corrections for the bilocal operators

$$\begin{aligned}
\gamma_\nu \gamma_\mu P_R \otimes \gamma^\nu \gamma^\mu P_L &= (4 + a_5 \epsilon) P_R \otimes P_L + E_5[O], \\
\gamma_\rho \gamma_\nu \gamma_\mu P_R \otimes \gamma^\rho \gamma^\nu \gamma^\mu P_L &= (4 + a_3 \epsilon) \gamma_\mu P_R \otimes \gamma^\mu P_L + E_3[O], \\
\gamma_\alpha \gamma_\rho \gamma_\nu \gamma_\mu P_R \otimes \gamma^\alpha \gamma^\rho \gamma^\nu \gamma^\mu P_L &= ((4 + a_5 \epsilon)^2 + b \epsilon) P_R \otimes P_L + E_7[O], \\
(\bar{s}^\alpha P_L d^\beta) (\bar{s}^\beta P_R d^\alpha) + 1/2 Q_1^{LR} &= E_1[O], \\
(\bar{s}^\alpha \gamma_\mu \gamma_\nu P_L d^\beta) (\bar{s}^\beta \gamma^\mu \gamma^\nu P_R d^\alpha) + (4 + a_5 \epsilon)/2 Q_1^{LR} &= E_6[O]. \tag{55}
\end{aligned}$$

In the equations for  $E_{1,6}$   $\alpha$  and  $\beta$  are colour indices. Note that the quark fields have been written explicitly only for these two evanescent operators which involve both colour singlet and anti-singlet operators. In all other cases the operators are colour singlets and each choice of colour structure and external quark fields define a particular evanescent operator. Most of these definitions can be found in Ref. [36]. As discussed in Ref. [34], the definition of these evanescent operators is not unique (as illustrated by the presence of arbitrary constants  $a_i$ ) and one has to ensure that one uses the same definitions in all steps of the calculation, so that the physical observables are independent of this choice. The definition of  $E_7[O]$  has been chosen in relation with that of  $E_5[O]$ , introducing a coefficient  $b$  in addition to the coefficient  $a_5$  introduced for the latter. This is a consistent choice for the two evanescent operators since  $E_7[O]$  may be seen as the evanescent operator coming from an evanescent operator (for instance, when inserting  $E_5[O]$  in loop diagrams). It was shown in Ref. [34] that such a consistent scheme led the anomalous dimensions to be independent of  $b$ .

A few more evanescent operators will be relevant in the four-quark theory when we dress the  $|\Delta S| = 2$  operators  $Q_{1,2}$  with gluons. These are written in a similar way as the previous ones up to a factor  $m_c^2/g^2$  multiplying the Dirac structure (see the end of Sec. 1.1). For instance one has for  $\hat{E}_5[Q]$  and  $\hat{E}_1[Q]$ :

$$\begin{aligned}
\frac{m_c^2}{g^2} (\gamma_\nu \gamma_\mu P_R \otimes \gamma^\nu \gamma^\mu P_L) &= \frac{m_c^2}{g^2} (4 + \tilde{a}_5 \epsilon) P_R \otimes P_L + \hat{E}_5[Q], \\
\frac{m_c^2}{g^2} (\bar{s}^\alpha P_L d^\beta) (\bar{s}^\beta P_R d^\alpha) + 1/2 Q_1 &= \hat{E}_1[Q], \tag{56}
\end{aligned}$$

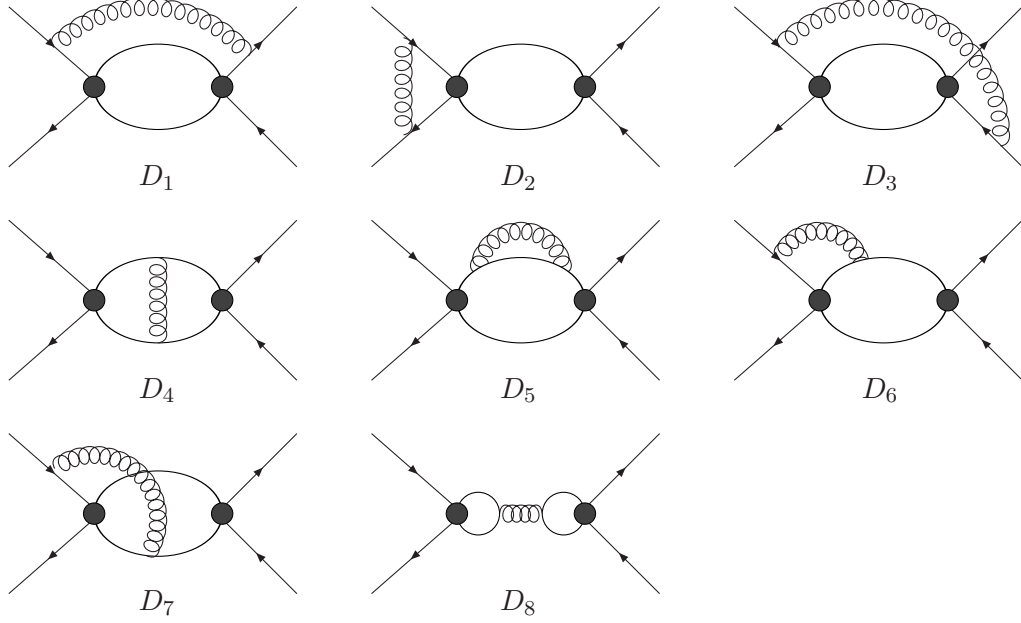


Figure 4: Diagrams  $D_i$  contributing at  $\mathcal{O}(\alpha_s)$  to the operators  $O_{ij}$  in the effective four flavour theory. The curly lines denote gluons and the black circles the insertions of  $|\Delta S| = 1$  current-current operators.

where the parameter of the  $\epsilon$  term is denoted with a tilde since its value does not need to be the same as the one used in Eq. (55) and the same is true for the other evanescent operators (in the following we use  $\tilde{a}_i = a_i$  for simplicity). Finally when evaluating loop diagrams with the insertion of QCD counterterms we will need the following evanescent operator:

$$\gamma_\rho \gamma_\nu \gamma_\mu P_L \otimes \gamma^\rho \gamma^\nu \gamma^\mu P_L = (16 + a_2 \epsilon) \gamma_\mu P_L \otimes \gamma^\mu P_L + E_2[O]. \quad (57)$$

In order to check our results we have thus performed the calculation for arbitrary values of  $a_i$  and  $b$ . However, unless specified and for simplicity, we will quote our results for

$$a_5 = 4, \quad a_3 = 4, \quad b = 96, \quad a_2 = -4. \quad (58)$$

Indeed, these values have been used in the determination of the anomalous dimensions [36] which were relevant for the renormalisation group calculations of the Wilson coefficients recalled in App. B, and choosing different  $a_i$  would require us to recompute these anomalous dimensions with the corresponding set of evanescent operators. Moreover, Fierz transformation can be applied in  $D$  dimensions with the choice  $a_5 = a_3 = 4$ .

The NLO QCD corrections will correspond to two different kinds of diagrams: first, the one-loop diagram involving two  $|\Delta S| = 1$  operators and leading to the operators  $O_{ij}$  can be dressed with a gluon (Fig. 4), then the  $|\Delta S| = 2$  local operators (counterterms or evanescent operators) can also be dressed (Fig. 5). We will consider both types of contributions in the following.

### 3.1.2 Calculation of the diagrams $D_i$

The diagram in Fig. 3 gives at one loop

$$D_0 = i \frac{m_c^2}{16\pi^2} \left( \frac{1}{\epsilon} - \log \left( \frac{m_c^2}{\mu^2} \right) - 1 - \frac{a_5}{4} \right) (P_R \otimes P_L + \tau_{rl} \gamma_\mu P_R \otimes \gamma^\mu P_L) + \dots \quad (59)$$

where the infinite part has been kept to demonstrate the need for the counterterms in Eq. (52).  $\tau_{rl}$  is defined in Eq. (42) where  $r, l$  are equal to  $\pm 1$  depending on the operator  $O_{rl}$  considered. The

dots contain the evanescent operators  $E_1$ ,  $E_5$  and  $E_6$  which appear in the computation of  $D_0$  in  $D$  dimensions in the NDR scheme. The two antisinglets  $E_1$  and  $E_6$  are needed to translate the antisinglet operators into  $\gamma_\mu P_R \otimes \gamma^\mu P_L$  while  $E_5$  appears in the calculation of  $D_0$  as can be seen from the presence of the term  $a_5$  in Eq. (59). Since these operators contribute to  $D_0$  at  $\mathcal{O}(1/\epsilon)$  as

$$D_0^E = -i \frac{m_c^2}{64\pi^2} \frac{1}{\epsilon} \left( E_5 + 2\tau_{rl}(-E_6 + 8E_1) \right), \quad (60)$$

they must be introduced as counterterms  $H_E \propto -D_0^E$  in Eq. (52) to regularise  $D_0$  in  $D$  dimensions. It is important to keep track of these operators: they contribute at two loops even in four dimensions, since their one-loop matrix element yield contributions proportional to the physical operators  $Q_i$  (see below).

The LO contribution to the part of the amplitude proportional to the Wilson coefficient  $C_{ij}$  in the effective four-quark theory Eq. (52) reads

$$\langle A^{(WW')}(μ) \rangle = 8G_F^2 β h^2 λ_c^{LR} λ_c^{RL} \sum_{i,j=+,-} C_{ij}(μ) \langle O_{ij}(μ) \rangle^{(0)}, \quad (61)$$

with

$$\langle O_{ij}(μ) \rangle^{(0)} = \frac{m_c^2(μ)}{4π^2} \left( 2 + \log\left(\frac{m_c^2}{μ^2}\right) \right) \sum_{k=1,2} τ_k^{ij} \langle Q_k^{LR}(μ) \rangle^{(0)}, \quad (62)$$

with  $τ_k^{ij}$  defined in Eq. (42) and from now on we use the value  $a_5 = 4$ . We can match this expression with Eq. (29) at the high scale  $μ_W$  (the value to be chosen for  $μ_W$  will be discussed in Sec. 3.5), using the fact that  $C_{ij}(μ_W) = 1$  at LO and  $\sum_{ij} τ_{ij} = 0$ , which leads to the NLO values of the Wilson coefficients  $C_i^r$  defined in Eq. (52):

$$\begin{aligned} C_1^r(μ_W) &= \mathcal{O}(α_s^2), \\ C_2^r(μ_W) &= -\frac{α_s(μ_W)}{4π} \times 4 \left[ 1 + \log\left(\frac{M_W^2}{μ_W^2}\right) - \frac{1}{4}(\log β + F(ω)) \right] + \mathcal{O}(α_s^2), \end{aligned} \quad (63)$$

with  $F(ω)$  given in Eq.(51).

We can now focus on the finite parts of the two-loop diagrams in Fig. 4, including the QCD counterterms required to renormalise the local  $|\Delta S| = 1$  operators. The results for the individual diagrams are given in App. D, adding up to

$$\langle O_{rl}(μ) \rangle^{(1)} = \langle O_{rl}(μ) \rangle^{(0)} - \frac{m_c^2(μ)}{64\pi^2} \frac{α_s(μ)}{4π} \sum_{i=1}^2 (\langle Q_i(μ) \rangle^{(0)} d_i^{rl}(μ) + \dots), \quad (64)$$

with

$$\begin{aligned}
Nd_1^{rl}(\mu) &= e_1^{rl}(\mu) + \xi \left[ \log \left( \frac{m_c^2}{\mu^2} \right) \right. \\
&\quad \left( (N + 2\tau_{rl}) \log \left( \frac{m_d^2 m_s^2}{\mu^4} \right) + R (4(N^2 - 2)\tau_{rl} - 2N) - 2(2N^2 + N - 4)\tau_{rl} + 2N - 1 \right) \\
&\quad + \left( (4 - N)\tau_{rl} + 2N - \frac{1}{2} \right) \log \left( \frac{m_d^2 m_s^2}{\mu^4} \right) + R_2 (2(N^2 - 2)\tau_{rl} - N) + R (4(N^2 - 2)\tau_{rl} - 2N) \\
&\quad \left. + \left( \frac{1}{3} (\pi^2 - 12) N^2 - N - \frac{\pi^2}{3} + 8 \right) \tau_{rl} + T \left( \frac{N}{2} + \tau_{rl} \right) + 2N - \frac{1}{2} \right], \tag{65}
\end{aligned}$$

$$\begin{aligned}
Nd_2^{rl}(\mu) &= e_2^{rl}(\mu) + \xi \left[ \log \left( \frac{m_c^2}{\mu^2} \right) \right. \\
&\quad \left( (4N\tau_{rl} + 2) \log \left( \frac{m_d^2 m_s^2}{\mu^4} \right) + R (4(N^2 - 2) - 8N\tau_{rl}) - 2(2N^2 + N - 4) + (8N - 4)\tau_{rl} \right) \\
&\quad + ((8N - 2)\tau_{rl} - N + 4) \log \left( \frac{m_d^2 m_s^2}{\mu^4} \right) + R (4(N^2 - 2) - 8N\tau_{rl}) + R_2 (2(N^2 - 2) - 4N\tau_{rl}) \\
&\quad \left. + \frac{1}{3} (\pi^2 - 12) N^2 + (2N(T + 4) - 2)\tau_{rl} - N + T - \frac{\pi^2}{3} + 8 \right]. \tag{66}
\end{aligned}$$

$\xi = 0$  corresponds to the gauge-independent results,  $T = \log^2(m_d^2/\mu^2) + \log^2(m_s^2/\mu^2)$  and  $\beta_{rl} = l + r$ . The gauge-independent parts  $e_i^{rl}(\mu)$  are given by:

$$\begin{aligned}
e_1^{rl}(\mu) &= \log \left( \frac{m_c^2}{\mu^2} \right) (-11(N^2 - 2)\beta_{rl} + (8N^2 - 6N + 16)\tau_{rl} - 16N - 12R\tau_{rl} - 3) \\
&\quad + \log^2 \left( \frac{m_c^2}{\mu^2} \right) (3(N^2 - 2)\beta_{rl} + 6N^2\tau_{rl} + 6N) + \left( (9 - 3N)\tau_{rl} + \frac{3}{2}(3N - 1) \right) \log \left( \frac{m_d^2 m_s^2}{\mu^4} \right) \\
&\quad + R((6N^2 - 2)\tau_{rl} - 3N) - 6R_2\tau_{rl} \\
&\quad + \frac{3}{4}(N^2 - 2)\beta_{rl} + \left( -\frac{41N^2}{2} - 7N - \pi^2 + 17 \right) \tau_{rl} + \frac{1}{2}(17N - 7), \tag{67}
\end{aligned}$$

$$\begin{aligned}
e_2^{rl}(\mu) &= \log \left( \frac{m_c^2}{\mu^2} \right) (R(12(N^2 - 1) - 24N\tau_{rl}) + 22N\beta_{rl} + (48N - 12)\tau_{rl} - 2(N(2N + 3) + 14)) \\
&\quad + \log^2 \left( \frac{m_c^2}{\mu^2} \right) (-6N\beta_{rl} + 12N\tau_{rl} + 12) + ((18N - 6)\tau_{rl} - 3N + 9) \log \left( \frac{m_d^2 m_s^2}{\mu^4} \right) \\
&\quad + R(-4N^2 + 8N\tau_{rl} - 2) + R_2(6(N^2 - 1) - 12N\tau_{rl}) \\
&\quad - \frac{3N\beta_{rl}}{2} - ((7 + 2\pi^2)N + 14)\tau_{rl} + N((\pi^2 - 3)N - 7) - \pi^2 + 20, \tag{68}
\end{aligned}$$

where  $R$  and  $R_2$  are infrared regularisations involving  $m_d$  and  $m_s$ , defined in App. D.

### 3.1.3 Calculation of the diagrams $L_i$

The diagrams  $L_i$  have two types of contributions depending on the operators involved.

- Contribution from the operators  $Q_i$

The three diagrams of Fig. 5 have to be evaluated with insertions of the operators  $Q_i$  ( $i = 1, 2$ ) defined in Eq. (53). The Wilson coefficients multiplying these operators receive two contributions given in Eq. (54). The calculation of  $C_i^r \langle Q_i \rangle$  is identical to the calculation of the corresponding local operators  $\tilde{C}_i \langle \tilde{Q}_i \rangle$  in the effective three-quark theory, and the results will be given in Sec. 3.2.

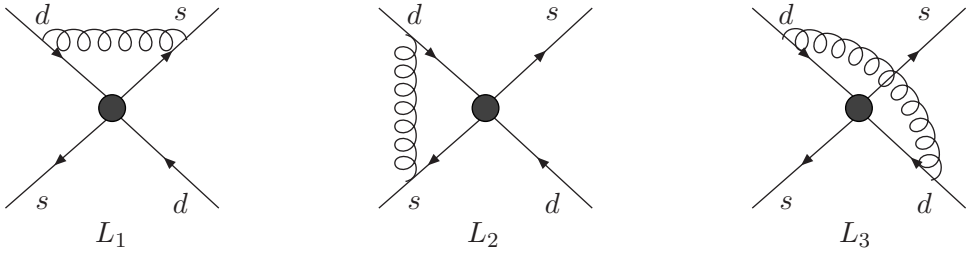


Figure 5: *Diagrams  $L_i$  contributing at  $\mathcal{O}(\alpha_s)$  in the effective four flavour theory. The curly lines denote gluons and the black circles the insertions of  $|\Delta S| = 2$  local operators.*

We can thus focus on the contribution from  $C_i^{\text{inf}}/\epsilon \langle Q_i \rangle$ , obtained by inserting the operator  $Q_i/\epsilon$  in the vertex of Fig. 5. The result, diagram by diagram, is given in App. D.2. Considering also the other members of each class of diagrams obtained by left-right and up-down reflections, we get

$$\langle Q_i(\mu) \rangle^{(1)} = \langle Q_i(\mu) \rangle^{(0)} + \frac{\alpha_s(\mu)}{4\pi} \sum_j \left( \frac{h_{Q_i}}{\epsilon} \delta_{ij} + b_{ji}(\mu) \right) \langle Q_j(\mu) \rangle^{(0)}. \quad (69)$$

The divergent parts will be discussed in Sec. 3.4 the elements  $(ij)$  of the gauge-independent finite part of the matrix  $4Nb(\mu)$  are given by

$$\begin{aligned} (11) &= -3(N+1) \log \left( \frac{m_d^2 m_s^2}{\mu^4} \right) + 2(3N^2 - 1) R - 6R_2 - 5N^2 + 11N - \pi^2 + 8, \\ (12) &= -\frac{3}{2}(N+1) \log \left( \frac{m_d^2 m_s^2}{\mu^4} \right) - 3NR + 6N + \frac{5}{2}, \\ (21) &= -6(N+1) \log \left( \frac{m_d^2 m_s^2}{\mu^4} \right) + 8NR - 12NR_2 + 2((3 - \pi^2)N + 11), \\ (22) &= -3(N+1) \log \left( \frac{m_d^2 m_s^2}{\mu^4} \right) - 2(2N^2 + 1) R + 6(N^2 - 1) R_2 + N(4N + 5) + 8 + \pi^2(N^2 - 1), \end{aligned} \quad (70)$$

and the gauge-dependent ones by

$$\begin{aligned} (11) &= \xi \left( T - N \log \left( \frac{m_d^2 m_s^2}{\mu^4} \right) + 4(2 - N^2) R + 2(N^2 - 2) R_2 + N(4N + 5) - 8 + \frac{\pi^2}{3}(N^2 - 1) \right) \\ (12) &= \xi \left( \frac{N}{2}T - \frac{1}{2} \log \left( \frac{m_d^2 m_s^2}{\mu^4} \right) + 2NR - NR_2 - 2N + \frac{3}{2} \right), \\ (21) &= \xi \left( 2NT - 2 \log \left( \frac{m_d^2 m_s^2}{\mu^4} \right) + 8NR - 4NR_2 - 8N + 10 \right), \\ (22) &= \xi \left( T - N \log \left( \frac{m_d^2 m_s^2}{\mu^4} \right) + 4(2 - N^2) R + 2(N^2 - 2) R_2 + N(4N + 3) - 8 + \frac{\pi^2}{3}(N^2 - 1) \right). \end{aligned} \quad (71)$$

### • Contribution from the evanescent operators

The contribution of the evanescent operators  $E_{1,3,5}$  introduced in the Hamiltonian  $H_E$  has also to be evaluated. In principle, a finite contribution could be added to these evanescent operators in the same way as for the  $C_i$ , Eq. (54). However, as indicated earlier, it has been shown in Refs. [34, 52] that the result should not depend on the value of the constant coefficients and that one can choose a regularisation scheme where these contributions cancel. Summing all the diagrams  $L_i$  together with

all the members of the same class (not shown, obtained by left-right and up-down reflections) one gets both finite and infinite parts. The finite parts are

$$\begin{aligned}
L_E^{(1)} &= \frac{1}{2N} \left( 3 + 2N + \xi \right) \langle Q_2 \rangle^{(0)} + \frac{1}{4} (2N + 3 + \xi) \langle Q_1 \rangle^{(0)}, \\
L_E^{(6)} &= 12 \left( \log \left( \frac{m_d^2 m_s^2}{\mu^4} \right) + 2R + \frac{1}{2N} - \frac{5}{3} + \frac{1}{6N} \xi \right) \langle Q_2 \rangle^{(0)} \\
&+ \left( \frac{6}{N} \log \left( \frac{m_d^2 m_s^2}{\mu^4} \right) + \frac{12}{N} R + 14N - \frac{24}{N} + 3 + \xi \right) \langle Q_1 \rangle^{(0)}, \\
L_E^{(5)} &= \frac{12}{N} \left( -\log \left( \frac{m_d^2 m_s^2}{\mu^4} \right) + 2(N^2 - 1)R - N^2 + 4 \right) \langle Q_2 \rangle^{(0)} - 6 \left( \log \left( \frac{m_d^2 m_s^2}{\mu^4} \right) - 3 \right) \langle Q_1 \rangle^{(0)},
\end{aligned} \tag{72}$$

whereas the combination of infinite parts does not cancel the ones coming from the  $D_i$  and  $C_i^{\text{inf}}$ s. They will be discussed below in relation with the anomalous dimensions necessary to determine the coefficients  $\bar{\eta}$ , see Eq. (93). One can already notice that all the logarithmic terms disappear once all contributions are summed up (an important test of the computation) and that by finally adding an additional QCD counterterm one obtains a regularised four-quark theory.

### 3.1.4 Final results

Adding up the two-loop calculation of the diagrams  $D_i$  and the contribution from the (evanescent and physical) counterterms, one finally gets for the effective four-quark theory

$$H(cc) = \frac{2G_F^2}{\pi^2} \beta h^2 m_c^2 \lambda_c^{LR} \lambda_c^{RL} \sum_i \left[ \sum_{rl} C_r C_l \left[ \left( 2 + \log \frac{m_c^2}{\mu^2} \right) \tau_i^{rl} + \frac{\alpha_s}{4\pi} c_i^{rl} \right] + C_i^r \right] Q_i + \dots \tag{73}$$

with

$$\begin{aligned}
4c_1^{rl} &= -\frac{3}{2} \log^2 \left( \frac{m_c^2}{\mu^2} \right) \left( \frac{(N^2 - 2) \beta_{rl}}{2N} + N \tau_{rl} + 1 \right) \\
&- 4 \log \left( \frac{m_c^2}{\mu^2} \right) \left( -\frac{11(N^2 - 2) \beta_{rl}}{16N} + \left( \frac{N}{2} + \frac{1}{N} - \frac{3}{8} \right) \tau_{rl} - \frac{3}{16N} - 1 \right) \\
&+ \frac{3}{N} \tau_{rl} R \left( 2 + \log \left( \frac{m_c^2}{\mu^2} \right) \right) \\
&- \frac{3(N^2 - 2) \beta_{rl}}{16N} - \frac{1}{8} \left( -71N + \frac{114}{N} - 24 \right) \tau_{rl} + \frac{3}{2N} - \frac{41}{8}, \tag{74}
\end{aligned}$$

$$\begin{aligned}
4c_2^{rl} &= -\frac{3}{N} R \left( (N^2 - 1) - 2N \tau_{rl} \right) \left( 2 + \log \left( \frac{m_c^2}{\mu^2} \right) \right) - 3 \log^2 \left( \frac{m_c^2}{\mu^2} \right) \left( \frac{1}{N} - \frac{\beta_{rl}}{2} + \tau_{rl} \right) \\
&- 4 \log \left( \frac{m_c^2}{\mu^2} \right) \left( 3 \left( 1 - \frac{1}{4N} \right) \tau_{rl} + \frac{1}{8} \left( -2N - \frac{14}{N} - 3 \right) + \frac{11\beta_{rl}}{8} \right) \\
&- 4 \left( \frac{43}{16} - \frac{3}{2N} \right) \tau_{rl} - \frac{1}{4} \left( -19N + \frac{60}{N} - 12 \right) + \frac{3\beta_{rl}}{8}, \tag{75}
\end{aligned}$$

and the values for  $C_i^r$  are given in Eq. (63). These gauge-independent terms have a remaining dependence on the regularisation through the  $R$  terms. The gauge-dependent terms are

$$\begin{aligned} 4c_{(1,\xi)}^{rl} &= -\left[ \left( \log \left( \frac{m_d^2 m_s^2}{\mu^4} \right) \left( \frac{1}{2} + \frac{\tau_{rl}}{N} \right) + \left( 1 - \frac{1}{2N} \right) + R \left( -1 + 2\tau_{rl} \left( N - \frac{2}{N} \right) \right) \right. \right. \\ &\quad \left. \left. + \tau_{rl} \left( -2N + \frac{4}{N} - 1 \right) \right) \left( 1 + \frac{1}{2} \log \left( \frac{m_c^2}{\mu^2} \right) \right) \right], \\ 4c_{(2,\xi)}^{rl} &= -\left[ \left( \log \left( \frac{m_d^2 m_s^2}{\mu^4} \right) \left( 2\tau_{rl} + \frac{1}{N} \right) + 2R \left( N - \frac{2}{N} - 2\tau_{rl} \right) \right. \right. \\ &\quad \left. \left. + \left( 2(2 - \frac{1}{N})\tau_{rl} - 2N - 1 + \frac{4}{N} \right) \right) \left( 1 + \frac{1}{2} \log \left( \frac{m_c^2}{\mu^2} \right) \right) \right]. \end{aligned} \quad (76)$$

It is interesting to notice that all the regularisation and gauge-dependent terms in Eqs. (74)-(76) are multiplied by the same quantity  $2 + \log(m_c^2/\mu^2)$  which is up to a constant the LO amplitude in the four-quark theory, Eq. (62). We will come back to this point while discussing the matching but it already indicates that these terms will cancel against similar terms from the effective three-quark theory in the final result.

### 3.2 Effective three-quark theory

Below the scale  $\mu_c \sim m_c$  the effective Hamiltonian is much simpler

$$H(cc) = \frac{2G_F^2}{\pi^2} \beta h^2 m_c^2(\mu) \lambda_c^{LR} \lambda_c^{RL} \sum_{i=1,2} \tilde{C}_i(\mu) \tilde{Q}_i^{LR}(\mu), \quad (77)$$

where the  $|\Delta S| = 2$  local operators  $\tilde{Q}_i^{LR}$  are defined as

$$\tilde{Q}_1^{LR} = (\bar{s}\gamma_\mu P_R d)(\bar{s}\gamma^\mu P_R d), \quad \tilde{Q}_2^{LR} = (\bar{s}P_L d)(\bar{s}P_R d). \quad (78)$$

They differ from the corresponding ones in the effective four-quark theory only through a normalisation. We need to determine  $\langle \tilde{Q}_i^{LR} \rangle$  in the effective three-quark theory at NLO:

$$\langle \tilde{Q}_i^{LR}(\mu) \rangle^{(1)} = \langle \tilde{Q}_i^{LR}(\mu) \rangle^{(0)} + \frac{\alpha_s(\mu)}{4\pi} \left( \sum_j a(\mu)_{ji} \langle \tilde{Q}_j^{LR}(\mu) \rangle^{(0)} + \dots \right), \quad (79)$$

and the ellipsis represents possible contributions from other operators. The structure is the same as discussed in the previous section, and one has for the first diagram  $L_1$

$$A^1 = \begin{pmatrix} -\frac{3}{2} + \xi(1-R) & 0 \\ 0 & 1 - 3R + \xi(1-R) \end{pmatrix}. \quad (80)$$

$A^2$  can be obtained from  $A^1$  by interchanging the diagonal elements. This can be understood easily, since  $L_2$  can be obtained from  $L_1$  by a Fierz transformation and the evanescent operators have been defined so as to conserve the Fierz relations. Evaluating  $L_3$  one gets

$$A^3 = \begin{pmatrix} -\frac{3}{2} + \xi \log \left( \frac{m_s^2}{\mu^2} \right) & -(3 + \xi)/4 \\ -3 - \xi & -\frac{3}{2} + \xi \log \left( \frac{m_s^2}{\mu^2} \right) \end{pmatrix}. \quad (81)$$

Adding up these three contributions and taking into account the colour factors (and the other members of each class obtained by left-right and up-down reflections) one finally gets:

$$a(\mu) = \begin{pmatrix} -\frac{3N^2-3N-4}{2N} + \frac{3}{N}R - \xi a_g & \frac{3(2N+1)}{4N} + \xi \frac{b_g}{4} \\ \frac{N+3}{N} + 6R + \xi b_g & \frac{2N^2+3N+4}{2N} - \frac{3(N^2-1)}{N}R - \xi a_g \end{pmatrix}, \quad (82)$$

with the gauge-dependent parts given by

$$\begin{aligned} a_g &= \frac{N^2 - 2}{N} R - \frac{2N^2 + N - 4}{2N} + \frac{1}{2N} \log \left( \frac{m_s^2 m_d^2}{\mu^4} \right), \\ b_g &= 2R - \frac{2N - 1}{N} - \log \left( \frac{m_s^2 m_d^2}{\mu^4} \right). \end{aligned} \quad (83)$$

The infinite parts of these diagrams are related to the LO anomalous dimensions of the operators  $\tilde{Q}_{1,2}^{LR}$  and  $Q_{1,2}^{LR}$ . We have checked that they agree with the ones obtained in Ref. [36].

### 3.3 Matching and Wilson coefficients

At NLO the matching of the effective four-quark theory, Eq. (52), to the three-quark theory, Eq. (77), at the scale  $\mu_c$  leads to

$$\tilde{C}_i(\mu_c) = \sum_{rl} C_r(\mu_c) C_l(\mu_c) \left( 2 + \log \left( \frac{m_c^2}{\mu_c^2} \right) \right) \tau_i^{rl} + C_i(\mu_c) \frac{\pi}{\alpha_s(\mu_c)}, \quad (84)$$

which we will use in the following. In addition, our results also provide an estimate of the size of NNLO corrections. Indeed, at NNLO several new contributions appear, one of them coming from the  $\mathcal{O}(\alpha_s)$  corrections to the operators discussed previously. In particular, the previous equation is modified as follows:

$$\tilde{C}_i^{\text{NNLO}}(\mu_c) = \sum_{rl} C_r(\mu_c) C_l(\mu_c) \left[ \left( 2 + \log \left( \frac{m_c^2}{\mu_c^2} \right) \right) \tau_{rl}^i + \frac{\alpha_s(\mu_c)}{4\pi} C_i^{\text{op}} \right] + \frac{\pi}{\alpha_s(\mu_c)} C_i(\mu_c) + \dots \quad (85)$$

with

$$C_i^{\text{op}} = c_i^{rl} - \frac{1}{8} \left( 2 + \log \left( \frac{m_c^2}{\mu_c^2} \right) \right) a_i^{rl}, \quad a_i^{rl} = \left( \tau_i^{rl} a_{ii}(\mu) + \tau_j^{rl} a_{ji}(\mu) \right), \quad (86)$$

and the dots stand for all other NNLO contributions. Using the expressions from Eq. (82) the  $a_i^{rl}$  read

$$\begin{aligned} a_1^{rl} &= \frac{6}{N} R \tau_{rl} - \left( 3N - \frac{4}{N} - 3 \right) \tau_{rl} + \frac{3}{2N} + 3 \\ &+ \xi \left[ - \left( \frac{1}{N} \tau_{rl} + \frac{1}{2} \right) \log \left( \frac{m_d^2 m_s^2}{\mu^4} \right) + R \left( 2\tau_{rl} \left( \frac{2}{N} - N \right) + 1 \right) + \tau_{rl} \left( 2N - \frac{4}{N} + 1 \right) + \frac{1}{2N} - 1 \right], \\ a_2^{rl} &= -6R \left( \frac{(N^2 - 1)}{N} - 2\tau_{rl} \right) + \frac{2(N + 3)}{N} \tau_{rl} + 2N + \frac{4}{N} + 3 \\ &+ \xi \left[ - \left( \frac{1}{N} + 2\tau_{rl} \right) \log \left( \frac{m_d^2 m_s^2}{\mu^4} \right) + 2R \left( -N + \frac{2}{N} + 2\tau_{rl} \right) \right. \\ &\left. + 2 \left( \frac{1}{N} - 2 \right) \tau_{rl} + 2N - \frac{4}{N} + 1 \right]. \end{aligned} \quad (87)$$

It is easy to check that the gauge-dependent terms as well as the terms involving small quark masses  $m_s$  and  $m_d$  are canceled at the matching scale  $\mu_c$  for any choice of the coefficients  $a_i$  in the definition of the evanescent operators. This provides powerful checks of the calculation and shows that our results are indeed independent of the choice of the QCD gauge and the infrared regularisation.

For completeness we give the final results in terms of  $a_2 = -4 + \epsilon_2$ ,  $a_3 = 4 + \epsilon_3$ ,  $a_5 = 4 + \epsilon_5$ ,  $\tilde{b} = 96 + \epsilon_b$ , where  $\epsilon_i = 0$  corresponds to the most widely used definitions of the evanescent operators

$$\begin{aligned}
8C_1^{\text{op}} &= \log\left(\frac{m_c^2}{\mu^2}\right) \left[ \epsilon_2 \left( \frac{(N^2-2)\beta_{rl}}{4N} + \left( \frac{1}{N} - N \right) \tau_{rl} + 1 \right) - \frac{\epsilon_3 \tau_{rl}}{N} - \frac{\epsilon_5}{2} \right. \\
&\quad \left. + \frac{11(N^2-2)\beta_{rl}}{2N} - \frac{(N^2+12)\tau_{rl}}{N} + 5 \right] + \log^2\left(\frac{m_c^2}{\mu^2}\right) \left( \left( \frac{3}{N} - \frac{3N}{2} \right) \beta_{rl} - 3N\tau_{rl} - 3 \right) \\
&\quad + \epsilon_5^2 \left( -\frac{(N^2-2)\beta_{rl}}{32N} + \left( \frac{3N}{16} - \frac{1}{4N} \right) \tau_{rl} - \frac{3}{16} \right) + \epsilon_b \left( \frac{3(N^2-2)\beta_{rl}}{64N} - \frac{(N^2-2)\tau_{rl}}{32N} + \frac{1}{8} \right) \\
&\quad + \epsilon_5 \left( \epsilon_2 \left( \frac{(N^2-2)\beta_{rl}}{16N} - \frac{(N^2-1)\tau_{rl}}{4N} + \frac{1}{4} \right) + \left( \frac{2}{N} - N \right) \beta_{rl} + \left( \frac{21N}{4} - \frac{11}{2N} \right) \tau_{rl} - \frac{45}{8} \right) \\
&\quad + \epsilon_2 \left( \left( \frac{N}{2} - \frac{1}{N} \right) \beta_{rl} + \left( \frac{2}{N} - 2N \right) \tau_{rl} + 2 \right) - \frac{\epsilon_3 \tau_{rl}}{N} \\
&\quad - \frac{3(N^2-2)\beta_{rl}}{8N} + \left( \frac{95N}{4} - \frac{73}{2N} \right) \tau_{rl} - \frac{65}{4}, \\
8C_2^{\text{op}} &= \log^2\left(\frac{m_c^2}{\mu^2}\right) \left( -\frac{6}{N} + 3\beta_{rl} - 6\tau_{rl} \right) \\
&\quad + \log\left(\frac{m_c^2}{\mu^2}\right) \left( \epsilon_2 \left( \frac{2}{N} - \frac{\beta_{rl}}{2} \right) - \frac{\epsilon_5}{N} - 2\epsilon_3\tau_{rl} + \frac{10}{N} - 11\beta_{rl} - 26\tau_{rl} \right) - 2\epsilon_3\tau_{rl} \\
&\quad + \epsilon_5 \left( -\frac{3(N^2+14)}{4N} + 2\beta_{rl} - \frac{\tau_{rl}}{2} \right) + \epsilon_5^2 \left( -\frac{3}{8N} + \frac{\beta_{rl}}{16} - \frac{\tau_{rl}}{8} \right) + \epsilon_b \left( \frac{1}{4N} - \frac{3\beta_{rl}}{32} + \frac{\tau_{rl}}{16} \right) \\
&\quad + \epsilon_2 \left( \epsilon_5 \left( \frac{1}{2N} - \frac{\beta_{rl}}{8} \right) + \frac{4}{N} - \beta_{rl} \right) + \frac{11N}{2} - \frac{38}{N} + \frac{3\beta_{rl}}{4} - \frac{51\tau_{rl}}{2}. \tag{88}
\end{aligned}$$

The physical observables should not depend on the values chosen for  $\epsilon_i$ . In the following, we will set  $\epsilon_i = 0$  since this is consistent with the values used for the anomalous dimensions.

### 3.4 Anomalous dimensions

In order to determine the short-distance QCD corrections in the EFT approach, we need to know the anomalous dimensions of all the operators involved. Most of them have been determined in Ref. [36]. However, in the case of  $\bar{\eta}_{cc}$ , we need to determine the anomalous dimensions  $\gamma_{rl,i}$  which enter the renormalisation group equations for the  $C_i$  and governs the mixing from double insertions into the  $C_i^r$ . Eq. (52) yields (see Ref. [35] for more detail)

$$\mu \frac{d}{d\mu} C_i^r(\mu) = \sum_j C_j^r(\mu) \gamma_{ji} + \sum_{r,l=+,-} C_r(\mu) C_l(\mu) \gamma_{rl,i}, \tag{89}$$

where

$$\gamma_{rl,i} = \frac{\alpha_s}{4\pi} \gamma_{rl,i}^{(0)} + \left( \frac{\alpha_s}{4\pi} \right)^2 \gamma_{rl,i}^{(1)} + \dots \tag{90}$$

The LO term  $\gamma_{rl,i}^{(0)}$  is given by

$$\gamma_{rl,i}^{(0)} = 8\tau_{rl,i}. \tag{91}$$

	$1/\epsilon$
$D_1$	$-2(6R - 7 + \xi(2R - 1))$
$D_2$	$\left( \left( 24 - \frac{\tilde{b}}{4} \right) \lambda + \frac{\tilde{b}}{4} + \xi(4 - 4R) - 30 \right)$
$D_3$	$\left( -3 + \frac{\tilde{b}}{8} + 2\xi \left( 2 \log \left( \frac{ms^2}{\mu^2} \right) + 1 \right) \right)$
$D_3(Q_1)$	$-(3 + \xi)$
$D_4$	$\left( \left( 48 - \frac{\tilde{b}}{2} \right) \lambda + \frac{\tilde{b}-72}{4} + 4\xi \right)$
$D_5$	$2(7 - \xi)$
$D_6$	$(-3 + 2\xi)$
$D_7$	$\left( \left( 24 - \frac{\tilde{b}}{4} \right) \lambda + \frac{\tilde{b}}{8} - 2\xi - 32 \right)$

Table 4: Divergences  $d_i, \tilde{d}_i$  of the two-loop diagrams for  $Q_2$  [apart from  $D_3(Q_1)$ ].  $\lambda$  multiplies the contribution from the evanescent operators which vanish for the standard value  $\tilde{b} = b = 96$ , see Eq. (58). The exact definition of the divergences can be found in Eq. (166).

The  $\gamma_{rl,i}^{(1)}$  are obtained from the  $1/\epsilon$  terms. The divergences from the diagrams in Fig. 4 are gathered in Tab. 4 while those from the counterterms  $C_i^{\text{inf}}$  yields contributions of the form  $h_i/\epsilon$ , see Eq. (69):

$$\begin{aligned}
h_{Q1} &= \frac{3R\tau_{rl}}{N} + \frac{1}{2} \left( \frac{4}{N} - 3N + 3 \right) \tau_{rl} + \frac{3}{4N} + \frac{3}{2} - \frac{\xi}{2} \left( \left( \frac{\tau_{rl}}{N} + \frac{1}{2} \right) \log \left( \frac{m_d^2 m_s^2}{\mu^4} \right) \right. \\
&\quad \left. + R \left( \left( 2N - \frac{4}{N} \right) \tau_{rl} - 1 \right) + \left( \frac{4}{N} - 2N - 1 \right) \tau_{rl} - \frac{1}{2N} + 1 \right), \\
h_{Q2} &= 3R \left( -N + \frac{1}{N} + 2\tau_{rl} \right) + N + \frac{2}{N} + \frac{3}{2} + \left( \frac{3}{N} + 1 \right) \tau_{rl} - \frac{\xi}{2} \left( \left( \frac{1}{N} + 2\tau_{rl} \right) \log \left( \frac{m_d^2 m_s^2}{\mu^4} \right) \right. \\
&\quad \left. + 2R \left( N - \frac{2}{N} - 2\tau_{rl} \right) - 2N + \frac{4}{N} - 1 + 2 \left( 2 - \frac{1}{N} \right) \tau_{rl} \right). \tag{92}
\end{aligned}$$

Finally the evanescent operators yield

$$\begin{aligned}
h_{E5,1} &= -12 + \frac{\tilde{b}}{4}, & h_{E5,2} &= -24N + \frac{\tilde{b}}{2N}, \\
h_{E1,1} &= 0, & h_{E1,2} &= 0, \\
h_{E6,1} &= -12N + \frac{\tilde{b}(N^2 - 2)}{8N}, & h_{E6,2} &= -\frac{\tilde{b} + 96}{4}. \tag{93}
\end{aligned}$$

As in the case of the two-loops diagrams, the divergence from the evanescent operator  $E_1$  cancels only for the standard values of  $a_i$ , Eq. (58). Combining these different contributions together one

gets

$$\begin{aligned}
-h^{rl,1}(\lambda) &= \frac{\lambda}{32N} \left( (\tilde{b} - 96) (N^2 - 2) \beta_{rl} + \left( 8(\tilde{b} - 48) - 6(\tilde{b} - 96)N^2 \right) \tau_{rl} + 6N(\tilde{b} - 80) \right) \\
&\quad - (\tilde{b} - 280) (N^2 - 2) \frac{\beta_{rl}}{64N} + \left( 3\tilde{b}N^2 - 4\tilde{b} - 152N^2 + 48 \right) \frac{\tau_{rl}}{32N} + \frac{1}{32}(376 - 3\tilde{b}), \\
-h^{rl,2}(\lambda) &= \frac{\lambda}{8N} \left( 3 \left( \tilde{b} - 16(N^2 + 4) \right) + \left( 48 - \frac{\tilde{b}}{2} \right) N\beta_{rl} + (\tilde{b} + 96) N\tau_{rl} \right) \\
&\quad + \frac{1}{16N}(-3\tilde{b} + 72N^2 + 304) + (\tilde{b} - 280) \frac{\beta_{rl}}{32} - \left( \frac{\tilde{b}}{8} + 13 \right) \frac{\tau_{rl}}{2}, \tag{94}
\end{aligned}$$

where the contribution from the evanescent operators is given with a factor  $\lambda$ . As discussed in Ref. [51], the correct contribution of evanescent operators to the NLO physical anomalous dimension matrix is obtained by inserting the evanescent counterterms with a factor of 1/2 instead of 1 into the one-loop diagrams. Hence the finite renormalisation terms from evanescent operators can be obtained by setting  $\lambda = 1/2$ :

$$\gamma_{rl,i}^{(1)} = -4h^{rl,i}(1/2). \tag{95}$$

It is easy to check that these anomalous dimensions are independent of  $\tilde{b}$  as demonstrated in Ref. [34]. This provides another important check of our calculation. In the case  $N = 3$  one obtains:

$$\begin{aligned}
\gamma_{++,1}^{(1)} &= -251/6, & \gamma_{+-,1}^{(1)} = \gamma_{-+,1}^{(1)} &= 169/2, & \gamma_{--,1}^{(1)} &= -355/6, \\
\gamma_{++,2}^{(1)} &= -41/3, & \gamma_{+-,1}^{(1)} = \gamma_{-+,2}^{(1)} &= 73/3, & \gamma_{--,2}^{(1)} &= 223/3. \tag{96}
\end{aligned}$$

In order to solve Eq. (89) we can rewrite the problem as a  $6 \times 6$  homogeneous renormalisation group equation

$$\mu \frac{d}{d\mu} \vec{D} = \tilde{\gamma}^T \cdot \vec{D}, \quad \vec{D} = \begin{pmatrix} C_r C_l \\ C_1 \\ C_2 \end{pmatrix}, \tag{97}$$

and solve for  $\vec{D}$  with

$$\tilde{\gamma}^T = \begin{pmatrix} (\gamma_r + \gamma_l) \cdot \mathbf{1}_4 & 0 \\ \gamma_{rl} & \gamma^T \end{pmatrix}, \quad \gamma_{rl} = \begin{pmatrix} \gamma_{++,1} & \gamma_{+-,1} & \gamma_{-+,1} & \gamma_{--,1} \\ \gamma_{++,2} & \gamma_{+-,2} & \gamma_{-+,2} & \gamma_{--,2} \end{pmatrix}, \tag{98}$$

and

$$\gamma^{(i)} = \begin{pmatrix} \hat{\gamma}_{LR,11}^{(i)} - 2(\gamma_m^{(i)} - \beta_i) & \hat{\gamma}_{LR,12}^{(i)} \\ \hat{\gamma}_{LR,21}^{(i)} & \hat{\gamma}_{LR,22}^{(i)} - 2(\gamma_m^{(i)} - \beta_i) \end{pmatrix}, \tag{99}$$

with  $\hat{\gamma}_{LR}^{(i)}$  the anomalous dimension at LO ( $i = 0$ ) or NLO ( $i = 1$ ) of the two  $|\Delta S| = 2$  operators  $Q_j^{LR}$  given in Eq. (144) and  $\beta_i$  the  $\beta$  functions which govern the evolution of the QCD coupling constant.  $\beta_0$  is given below Eq. (14) and  $\beta_1 = 102 - 38/3f$ .

### 3.5 EFT result

Combining Eq. (84) with the renormalisation equation for  $D$ , we obtain the final result for  $\bar{\eta}_{a,cc}^{(LR)}$  at NLO in the EFT approach, corresponding to the gauge-invariant combination of diagrams shown in the first row of Fig. 2:

$$\bar{\eta}_{a,cc}^{(LR)} = \frac{1}{S^{LR}(x_c, \beta, \omega)} \sum_{j=1,2} \left( \left( 1 + \frac{\alpha_s(\mu)}{4\pi} K^{[3]} \right) \exp \left[ d^{[3]} \cdot \log \frac{\alpha_s(\mu_c)}{\alpha_s(\mu)} \right] \left( 1 - \frac{\alpha_s(\mu_c)}{4\pi} K^{[3]} \right) \right)_{aj} F_j(\mu_c), \tag{100}$$

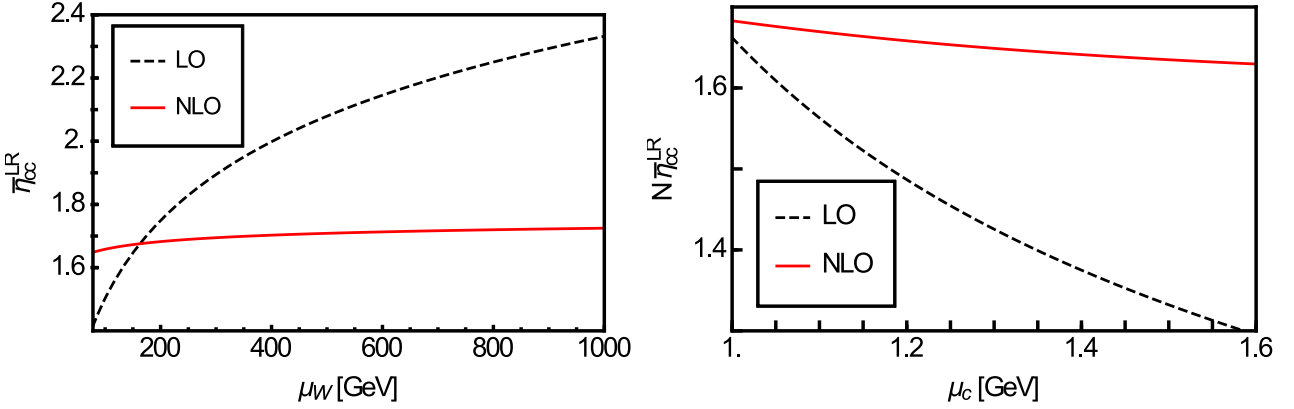


Figure 6: Dependence of  $\bar{\eta}_{cc}$  on the high (left panel) and on the low (right panel) scale in the EFT approach for  $M_{W_R} = 1000$  GeV and respectively for  $\mu_c = m_c$  and  $\mu_W = M_W$ . The other parameters are given in the text. The relevant quantity when  $\mu_c \neq m_c$  is  $N\bar{\eta}_{cc}$  with  $N$  defined in Eq. (110).

with  $S^{LR}(x_c, \beta, \omega)$  given in Eq.(50) and

$$\begin{aligned} F_a(\mu_c) &= \left( \frac{\pi}{\alpha_s(\mu_c)} C_a(\mu_c) + \sum_{r,l=+,-} \left( r_{rl,a}(\mu_c) + \frac{\alpha_s(\mu_c)}{4\pi} C_a^{\text{op}}(\mu_c) \right) C_r(\mu_c) C_l(\mu_c) \right), \quad (101) \\ r_{rl,a}(\mu_c) &= (2 + \log(m_c^2/\mu_c^2)) \tau_a^{rl}, \quad a = 1, 2, \end{aligned}$$

where the values of  $C_a(\mu_c)$ ,  $C_r(\mu_c)$  and  $C_l(\mu_c)$  are given by the evolution of  $D$  down to  $\mu_c$

$$\begin{aligned} \vec{D}(\mu_c) &= \left( 1 + \frac{\alpha_s(\mu_c)}{4\pi} \tilde{J}^{[4]} \right) \cdot \exp \left[ \tilde{d}^{[4]} \cdot \log \frac{\alpha_s(\mu_b)}{\alpha_s(\mu_c)} \right] \cdot \left( 1 + \frac{\alpha_s(\mu_b)}{4\pi} (\delta \tilde{r}^T(\mu_b) + \tilde{J}^{[5]} - \tilde{J}^{[4]}) \right) \\ &\cdot \exp \left[ \tilde{d}^{[5]} \cdot \log \frac{\alpha_s(\mu_W)}{\alpha_s(\mu_b)} \right] \cdot \left( 1 - \frac{\alpha_s(\mu_W)}{4\pi} \tilde{J}^{[5]} \right) \cdot \vec{D}(\mu_W). \quad (102) \end{aligned}$$

In order to get an estimate of the error due to neglected higher-order contributions, we have added in Eq. (101) the contribution  $C_a^{\text{op}}$  which first appears at the next order. The  $C_i^r(\mu_W)$  are defined in Eq. (63) while  $C_{\pm}(\mu_W)$  is defined in Eq. (126). The contribution  $\delta \tilde{r}^T(\mu_b)$  cancels in the absence of penguin operators, which we have neglected.

Finally the matrices  $\tilde{d} = \tilde{d}^{[f]}$ ,  $\tilde{J} = \tilde{J}^{[f]}$  and  $d = d^{[3]}$ ,  $K = K^{[3]}$  encode respectively the  $6 \times 6$  anomalous dimension matrix  $\tilde{\gamma}$  defined in Sec. 3.4 and the  $2 \times 2$  one  $\tilde{\gamma}_{LR}$  defined in App. B.2, with the additional definition

$$\tilde{d} = \frac{(\tilde{\gamma}^{(0)})^T}{2\beta_0}, \quad \tilde{J} + [\tilde{d}, \tilde{J}] = -\frac{(\tilde{\gamma}^{(1)})^T}{2\beta_0} + \frac{\beta_1}{\beta_0} \tilde{d}. \quad (103)$$

Simplified expressions for  $D_i(\mu_c)$  where effects from the five-flavour theory have been neglected and

which are extremely good approximations to the complete results read

$$\begin{aligned}
F_1 &= \frac{3}{104} \frac{\pi}{\alpha_s} (2A^{--} - 39A^{+-} - 26A^{++} + 63A_1) \\
&\quad - \frac{1}{8} \left( \log \left( \frac{m_c^2}{\mu_c^2} \right) + 2 \right) (A^{--} - 6A^{+-} + 5A^{++}) \\
&\quad + \frac{1}{4} \left( -\frac{1761281}{390000} A^{--} + \frac{587029}{220000} A^{+-} + \frac{16120889}{1110000} A^{++} - \frac{4789827}{260000} A_1 + \frac{1737}{296} A_2 \right. \\
&\quad + A \left( A^{--} \left( -\frac{12}{13} \log \left( \frac{\mu_W}{M_W} \right) - \frac{10181}{16250} \right) + A^{+-} \left( \frac{9}{2} \log \left( \frac{\mu_W}{M_W} \right) + \frac{39993}{10000} \right) \right. \\
&\quad \left. \left. + A^{++} \left( -6 \log \left( \frac{\mu_W}{M_W} \right) - \frac{7031}{2500} \right) + A_1 \left( \frac{63}{26} \log \left( \frac{\mu_W}{M_W} \right) - \frac{974889}{1430000} \right) \right) \right), \\
F_2 &= \frac{3}{1924} \frac{\pi}{\alpha_s} (2590A^{--} - 481A^{+-} - 182A^{++} + 777A_1 - 2704A_2) \\
&\quad + \frac{1}{4} \left( \log \left( \frac{m_c^2}{\mu_c^2} \right) + 2 \right) (A^{--} + 2A^{+-} + A^{++}) \\
&\quad + \frac{1}{4} \left( -\frac{101273}{9750} A^{--} + \frac{3969529}{330000} A^{+-} + \frac{6590729}{555000} A^{++} - \frac{5219109}{130000} A_1 + \frac{21963}{3700} A_2 \right. \\
&\quad + A \left( -\frac{7}{1625} A^{--} \left( 15000 \log \left( \frac{\mu_W}{M_W} \right) + 10181 \right) + A^{+-} \left( 3 \log \left( \frac{\mu_W}{M_W} \right) + \frac{13331}{5000} \right) \right. \\
&\quad \left. - \frac{7}{46250} \left( 15000 \log \left( \frac{\mu_W}{M_W} \right) + 7031 \right) A^{++} \right. \\
&\quad \left. + A_2 \left( 2 \log \left( \frac{M_W}{M_{W'}} \right) + F(\omega) - 8 \log \left( \frac{M_W}{\mu_W} \right) + \frac{2304}{37} \log \left( \frac{\mu_W}{M_W} \right) + \frac{1318747}{22200} \right) \right. \\
&\quad \left. + A_1 \left( \frac{21}{13} \log \left( \frac{\mu_W}{M_W} \right) - \frac{324963}{715000} \right) \right), \tag{104}
\end{aligned}$$

with

$$\begin{aligned}
A &= \frac{\alpha_s(\mu_W)}{\alpha_s(\mu_c)}, & A_1 &= \left( \frac{\alpha_s(\mu_W)}{\alpha_s(\mu_c)} \right)^{\frac{2}{25}}, & A_2 &= \left( \frac{\alpha_s(\mu_W)}{\alpha_s(\mu_c)} \right)^{-1}, \\
A^{++} &= \left( \frac{\alpha_s(\mu_W)}{\alpha_s(\mu_c)} \right)^{\frac{12}{25}}, & A^{+-} &= \left( \frac{\alpha_s(\mu_W)}{\alpha_s(\mu_c)} \right)^{-\frac{6}{25}}, & A^{--} &= \left( \frac{\alpha_s(\mu_W)}{\alpha_s(\mu_c)} \right)^{-\frac{24}{25}}. \tag{105}
\end{aligned}$$

The value of  $\bar{\eta}_{cc}^{(LR)} \equiv \bar{\eta}_{2,cc}^{(LR)}$  at the scale  $\mu = 1$  GeV is

$$\bar{\eta}_{cc}^{(LR)} \Big|_{EFT} = \frac{1}{1 - 0.0294 F(\omega)} [1.562 - 0.473 + (0.604 - 0.037 F(\omega))], \tag{106}$$

with  $F(\omega)$  defined in Eq. (51), and we have taken  $M_{W'} = 1$  TeV (we will see below that the dependence on this parameter is very weak). We are now in a position to compare the EFT result with the method of region. For  $\omega = 0.1$  ( $\omega = 0.8$ ) we get from the previous equation

$$\bar{\eta}_{cc}^{(LR)} \Big|_{EFT} = 1.41 + 0.67 - 0.43 = 1.65 \quad (3.41 - 0.17 - 1.03 = 2.21). \tag{107}$$

We add the contributions given in Table 2 for the three diagrams 2 (a)+(b)+(c) with the appropriate weights, and we normalise the result to  $S^{LR}(x_c, \beta, \omega)$  in order to be able to directly compare with the EFT result

$$\bar{\eta}_{cc}^{(LR)} \Big|_{MR} = 1.50 + 0.13 - 0.25 = 1.37 \quad (1.76 + 0.25 - 0.50 = 1.51). \tag{108}$$

As in the SM case, we see that the results from the MR are only in broad agreement (around 30%) with the EFT approach in the presence of large logarithms, and we will take the EFT NLO estimate as our central value. Our final result at the scale  $\mu = 1$  GeV and for  $\omega = 0.1$  ( $\omega = 0.8$ ) is

$$\bar{\eta}_{cc}^{(LR)} = 1.65 \pm 0.33 \quad (2.21 \pm 0.44), \quad (109)$$

where the conservative 20% error bar takes into account our estimation of higher-order terms: the contribution from  $C_a^{op}$  (which turns out to be very small), contributions from the expansion of Eq. (100) up to NNLO, the expected size of NNLO terms assuming a geometrical growth between LO, NLO and NNLO contributions, the possibility to set  $\mu_W$  at two different high scales ( $M_W$  and  $M_{W'}$ ) when integrating out the  $W$  and  $W'$  bosons to match onto the four-flavour theory, the dependence on the choice of the matching scales (for the matching onto the three-flavour theory). Each of these errors are of the order of a few percent. Furthermore we neglected the effect of resumming the contributions  $\log \beta$ . This last error is clearly difficult to determine without an explicit calculation, however we will see below that this uncertainty is small in other cases ( $ct$  and  $tt$  boxes) with the MR, suggesting that the error should be smaller than our conservative estimate of 20%.

The dependence on the different matching scales  $\mu_W$  and  $\mu_c$  is illustrated on Fig. 6. This illustrates the strong dependence of the LO result on the matching scales and the much milder dependence at NLO. This behaviour is similar to what is observed in the SM [29, 33, 35] and it constitutes another significant check of our computation. In the case of the dependence on  $\mu_c$ , the relevant quantity is  $N\bar{\eta}_{cc}$  with the normalisation factor given by

$$N = S^{LR}(x_c(\mu_c))/S^{LR}(x_c(m_c)), \quad (110)$$

considering that the quantity which multiplies  $\bar{\eta}_{cc}^{(LR)}$  in the Hamiltonian is  $S^{LR}(x_c(m_c))$ . We also show the dependence on the choice of the hadronic scale  $\mu_h$  on the left panel of Fig. 7 for typical values between  $1 < \mu_h < 2$  GeV. As can be seen on the right panel of the same figure, there is a very mild dependence on the ratio of the masses of the  $W'$  and  $H$  bosons at NLO.

The above study shows that in the presence of large logarithms, the MR provides only an approximate value of the actual EFT result at NLO (around 30%). We now turn to  $ct$  or  $tt$  diagrams, which involve a contribution  $\log \beta$  which might either be considered as a large logarithm or not from the point of view of MR. We obtain

$$\bar{\eta}_{tt}^{(LR)} = 2.74 \pm 0.82 \pm 0.04 \quad (2.67 \pm 0.80 \pm 0.03), \quad (111)$$

$$\bar{\eta}_{ct}^{(LR)} = 5.88 \pm 1.76 \pm 0.23 \quad (5.34 \pm 1.60 \pm 0.10), \quad (112)$$

where the central value and the second uncertainty are obtained by considering the values obtained with or without a resummation of  $\log \beta$ , and the first error is a 30% estimate of the uncertainty of the MR in the presence of the potentially large logarithm  $\log \beta$ .

As indicated earlier, resumming or not  $\log \beta$  yields a small uncertainty from a few percent in both cases. Moreover, we can see that our result is very stable with respect to  $\omega$ .

## 4 Conclusion

Among the extensions of the Standard Model, Left-Right models provide an interesting solution to the violation of parity coming from the weak interaction. These models exhibit both additional  $W'$  and  $Z'$  gauge bosons and an extended Higgs sector needed to trigger the breakdown of the left-right symmetry. They are significantly constrained by several kinds of observables, and in particular kaon mixing which is accurately measured and which gets contributions from tree-level neutral Higgs inducing flavour-changing neutral currents.

Kaon mixing can be analysed in the framework of the effective Hamiltonian, separating short- and long-distance contributions. The latter yield matrix elements that can be evaluated at a hadronic

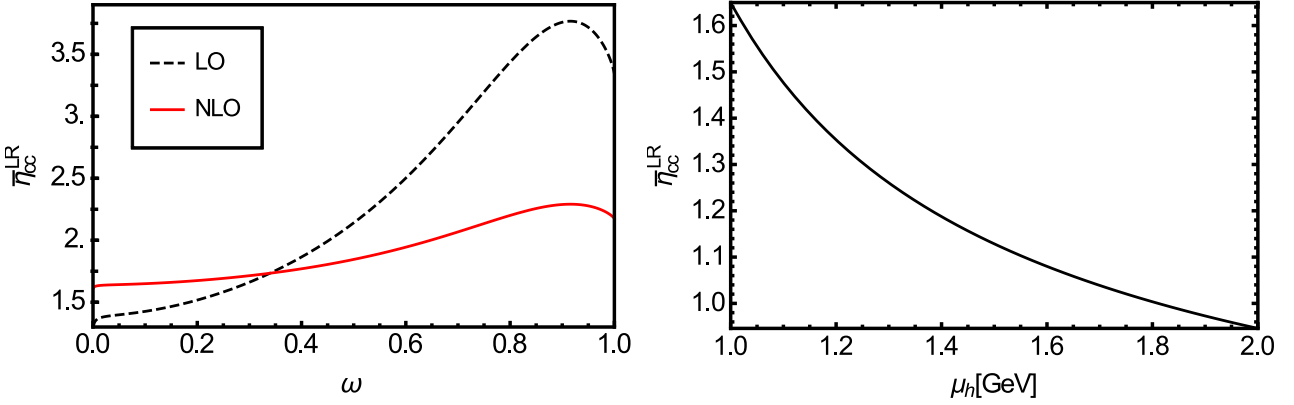


Figure 7: Dependence of  $\bar{\eta}_{cc}$  on  $\omega = M_{W'}^2/M_H^2$  (left panel) and on the hadronic scale  $\mu_h$  (right panel) in the EFT approach.

scale of a few GeV using lattice QCD simulations. The short distance contributions can be determined thanks to a matching onto the fundamental theory (SM or Left-Right model) at a high scale corresponding to the mass of the heavy degrees of freedom. The bridge between the two scales is provided by RGE, which allows one to perform a resummation of large logarithms stemming from QCD corrections.

These short-distance QCD corrections are relevant to compute kaon mixing accurately in the Standard Model. They have been computed in the SM using a rigorous EFT approach where heavy degrees of freedom are progressively integrated out as the scale is lowered, showing the importance of NLO corrections. Another, approximate, method has been devised in earlier times to compute these QCD corrections at LO, consisting in determining the range of loop momenta responsible for the large logarithms and introducing the relevant anomalous dimensions to resum these logarithms. This method of regions is admittedly approximate but is far less demanding in terms of computation, compared to the EFT approach.

We first recalled basic features of these two methods, before proposing an extension of the method of regions to include NLO corrections. We compared the results of the two methods in the case of the Standard Model, finding a good agreement for SM diagrams dominated by a single mass, but a 30% discrepancy between our extension of the method of regions and the EFT computation in the case of large logarithm. We then considered the corrections for the Left-Right models using the method of regions. For some of the contributions, the computation has a different structure, depending on whether  $\log \beta$  is treated as a large logarithm or not.

Since the  $cc$  box exhibits a large logarithm  $\log x_c$  at LO and thus might suffer from a large uncertainty in the method of regions, we decided to compute the short-distance QCD correction within the EFT approach, following closely Refs. [33–36] (the computation for  $ct$  or  $tt$  would require a NLO matching at the high scale which has not been computed yet). We matched the LR model onto a four-flavour theory, which was run down to  $m_c$  and matched onto a three-flavour theory, before reaching a low hadronic scale  $\mu_h$ . A large number of cross-checks have been performed on our results (independence of the QCD gauge, independence of the definition of the evanescent operators, independence of the infrared regulators). Our result for  $\bar{\eta}_{cc}^{(LR)}$  at NLO in the EFT approach showed again a 30% discrepancy with the method of regions. We finally provided an estimate of the uncertainty to attach to our EFT computation at NLO.

We considered also the case of  $ct$  and  $tt$  boxes, where another logarithm, namely  $\log \beta$ , may or may not be considered as large. Within the method of regions, both cases led to very similar results. We then provided estimates for  $\eta_{ct}^{(LR)}$  and  $\eta_{tt}^{(LR)}$  at NLO, using conservative error estimates based on our previous comparisons between the two approaches.

These results can be extended to the mixing for  $B_d$  and  $B_s$  meson, and they can be used in

order to constrain Left-Right models. Other constraints, such as electroweak precision observables, flavour-changing charged currents and direct searches, have also proven important and call for a global analysis of these models within an appropriate statistical framework. This will be the object of future work to determine the viability of Left-Right models, their ability to solve the violation of parity occurring in the Standard Model and the possibility to find part of their spectrum in the next run of the LHC [49].

## Acknowledgments

We would like to thank M. Knecht and H. Sadzjian for interesting and useful discussions. LVS acknowledges funding by the P2IO LabEx (ANR-10-LABX-0038) in the framework “Investissements d’Avenir” (ANR-11-IDEX-0003-01) managed by the French National Research Agency (ANR).

## A SM case at NLO with the method of regions

We want to apply the method of regions as explained in Sec. 1.2 in order to determine the short-distance corrections  $\bar{\eta}$  at NLO. We start with the behaviour of the one-loop integrals. In the SM these integrals are given by the following functions

$$\begin{aligned} S(x_t) &= x_t \left( \frac{1}{4} + \frac{9}{4} \frac{1}{1-x_t} - \frac{3}{2} \frac{1}{(1-x_t)^2} \right) - \frac{3}{2} \left[ \frac{x_t}{(1-x_t)} \right]^3 \log x_t, \\ S(x_c) &= x_c + \mathcal{O}(x_c^2), \\ S(x_c, x_t) &= -x_c \log x_c + x_c F(x_t) + \mathcal{O}(x_c^2 \log x_c), \quad F(x_t) = \frac{x_t^2 - 8x_t + 4}{4(1-x_t)^2} \log x_t + \frac{3}{4} \frac{x_t}{(x_t - 1)}. \end{aligned} \quad (113)$$

Clearly the leading behaviour of the one-loop integral for  $\bar{\eta}_{tt}$  is  $\mathcal{O}(1)$ , for  $\bar{\eta}_{cc}$   $\mathcal{O}(x_c)$  and for  $\bar{\eta}_{ct}$   $\mathcal{O}(x_c \log(x_c))$ . Following the method of regions, the remaining integration over the momentum  $k$  leads to  $m_t^2$  in the first case, and  $m_c^2$  in the second, as already discussed in Sec. 1.2. For  $ct$  one has to introduce the function  $R(\gamma, m_1, m_2)$  defined in Eq. (22) at LO. At NLO the quantity  $x_c F(x_t)$  contributes to  $\bar{\eta}_{ct}$ , so that the result of the integration is  $m_c^2$ , similarly to  $\bar{\eta}_{cc}$ .

One has then to determine the anomalous dimensions of the operators which appear in the calculation of the box diagrams. These anomalous dimensions are well known up to NLO, for instance see Ref. [36]. We have to multiply the anomalous dimensions of  $|\Delta S| = 1$  operators  $d_r$  and  $d_l$  between  $\mu_W^2$  and  $k^2$  with the anomalous dimension  $d_V$  of the  $|\Delta S| = 2$  operator between  $k^2$  and  $\mu_h$ . Setting  $k^2 = m_c^2$ , we obtain the following formula for the scale-independent correction  $\eta_{tt}$

$$\begin{aligned} \eta_{tt} &= \sum_{r,l=\pm} (\alpha_s(m_c))^{d_V^{(3)}} \left( \frac{\alpha_s(m_t)}{\alpha_s(\mu_5)} \right)^{d_V^{(5)}} \left( \frac{\alpha_s(\mu_5)}{\alpha_s(m_c)} \right)^{d_V^{(4)}} \left( \frac{\alpha_s(\mu_W)}{\alpha_s(m_t)} \right)^{d_r^{(5)} + d_l^{(5)}} a_{rl} \\ &\quad \left( 1 - \frac{\alpha_s(m_c)}{4\pi} (J_V^{(3)} - J_V^{(4)}) - \frac{\alpha_s(\mu_5)}{4\pi} (J_V^{(4)} - J_V^{(5)}) + \frac{\alpha_s(m_t)}{4\pi} (J_r^{(5)} + J_l^{(5)} - J_V^{(5)}) \right. \\ &\quad \left. - \frac{\alpha_s(\mu_W)}{4\pi} (J_l^{(5)} + J_r^{(5)} - B_r^{(5)} - B_l^{(5)}) \right), \end{aligned} \quad (114)$$

where exponents denote the number of active flavours,  $\mu_5$  is the threshold for the integration of the  $b$ -quark, and  $J$  arises from the RGE evolution as described in App. B. Note that in contrast to the EFT approach the operators  $O_{\pm}$  appear in the method of regions since one does not integrate the top quark in this method but rather one tries to capture the relevant features of the one-loop integrals.

For  $\eta_{ct}$ , we have two different types of contributions: a large logarithm  $\log x_c$  and a constant term. Since we want to resum contributions of the form  $\alpha_s \log x_c$ , the first can be formally counted

as coming one order earlier than the latter in the power counting. We can take this into account by treating differently the resummation of the large logarithm and the constant term

$$\begin{aligned} \eta_{ct} &= \frac{1}{-\log x_c + F(x_t)} \alpha_s(m_c)^{d_V} \sum_{r,l=\pm} a_{rl} \left( \frac{\alpha_s(\mu_W)}{\alpha_s(m_c)} \right)^{d_l+d_r} \\ &\quad \times \left( -\log x_c R_{\log}^{NLO} \left[ -d_l - d_r + d_V + 2d_m, u_{rl}, j_{rl}; m_c, \mu_W \right] + F(x_t) \right), \end{aligned} \quad (115)$$

with

$$\begin{aligned} a_{rl} &= [1 + r + l + 3rl]/4 \\ u_{rl} &= 1 + 2 \frac{\alpha_s(m_c)}{4\pi} J_m - \frac{\alpha_s(\mu_W)}{4\pi} (J_l + J_r - B_l - B_r), \\ j_{rl} &= J_l + J_r - J_V - 2J_m, \end{aligned} \quad (116)$$

and

$$R_{\log}^{NLO}(\gamma, U, J; m_1, m_2) = \log^{-1} \frac{m_2^2}{m_1^2} \left( \frac{\alpha_s(m_1)}{\alpha_s(\mu)} \right)^{-\gamma} \int_{m_1^2}^{m_2^2} \frac{dk^2}{k^2} \left( \frac{\alpha_s(k)}{\alpha_s(\mu)} \right)^\gamma \left[ U + \frac{\alpha_s(k)}{4\pi} J \right], \quad (117)$$

where  $U$  does not depend on  $k$ , yielding for  $\gamma \neq 0, 1$

$$\begin{aligned} R_{\log}^{NLO}(\gamma, U, J; m_1, m_2) &= \frac{1}{\log(m_2^2/m_1^2)} \frac{4\pi}{\beta_0 \alpha_s(m_1)} \\ &\quad \times \left[ \frac{1}{1-\gamma} \left\{ \left( \frac{\alpha_s(m_2)}{\alpha_s(m_1)} \right)^{\gamma-1} - 1 \right\} U + \frac{\alpha_s(m_1)}{4\pi} \frac{1}{\gamma} \left[ \frac{\beta_1}{\beta_0} U - J \right] \left\{ \left( \frac{\alpha_s(m_2)}{\alpha_s(m_1)} \right)^\gamma - 1 \right\} \right]. \end{aligned} \quad (118)$$

The previous cases, where a single mass scale  $m_1$  dominates the integral, can be described using the averaging function

$$R_1^{NLO}(\gamma, U, J; m_1, m_2) = \left[ U + \frac{\alpha_s(m_1)}{4\pi} J \right] \quad (119)$$

## B Operators and anomalous dimensions

### B.1 $|\Delta S| = 1$ operators

We have the  $|\Delta S| = 1$  vector operators for the SM case [35, 36]

$$O_1^{VLL} = (\bar{d}^\alpha \gamma_\mu P_L s^\beta)(\bar{V}^\beta \gamma^\mu P_L U^\alpha), \quad O_2^{VLL} = (\bar{d} \gamma_\mu P_L s)(\bar{V} \gamma^\mu P_L U), \quad (120)$$

$$O_1^{VLR} = (\bar{d} \gamma_\mu P_L s)(\bar{V} \gamma^\mu P_R U), \quad O_2^{VLR} = (\bar{d}^\alpha \gamma_\mu P_L s^\beta)(\bar{V}^\beta \gamma^\mu P_R U^\alpha), \quad (121)$$

where  $U$  and  $V$  can be any up-type fermions. As discussed in Ref. [36], Fierz identities hold for these operators up two loops in the NDR- $\overline{MS}$  scheme, as long as penguin operators are not included in the discussion. The anomalous dimensions for the vector-vector operators is simpler for [36]

$$O_\pm = \frac{O_1 \pm O_2}{2}, \quad (122)$$

which are the following

$$\begin{aligned} \gamma_\pm^{(0)} &= \pm 6 \frac{N \mp 1}{N}, & \gamma_\pm^{(1)} &= \frac{N \mp 1}{2N} \left( -21 \pm \frac{57}{N} \mp 19 \frac{N}{3} \pm \frac{4}{3} f \right), \\ \gamma_m^{(0)} &= 6C_F, & \gamma_m^{(1)} &= C_F \left( 3C_F + \frac{97}{3}N - \frac{10}{3}f \right), \end{aligned} \quad (123)$$

where the second line corresponds to the anomalous dimensions for masses with  $C_F = (N^2 - 1)/2N$ , and for  $N = 3$ ,  $\gamma_+^{(0)} = 4$ ,  $\gamma_-^{(0)} = -8$ ,  $\gamma_m^{(0)} = 8$ .

We introduce the correction of the anomalous dimensions

$$J_{\pm} = \frac{d_{\pm}\beta_1}{\beta_0} - \frac{\gamma_{\pm}^{(1)}}{2\beta_0}, \quad d_{\pm} = \frac{\gamma_{\pm}^{(0)}}{2\beta_0}, \quad (124)$$

$$J_m = \frac{d_m\beta_1}{\beta_0} - \frac{\gamma_m^{(1)}}{2\beta_0}, \quad d_m = \frac{\gamma_m^{(0)}}{2\beta_0}, \quad (125)$$

and the value of the Wilson coefficients at the high scale  $C_{\pm}(\mu_W)$  defined in Ref. [29]

$$C_{\pm}(\mu_W) = 1 + \frac{\alpha_s(\mu_W)}{4\pi} \left( \log \frac{\mu_W}{M_W} \gamma_{\pm}^{(0)} + B_{\pm} \right) + \mathcal{O}(\alpha_s^2), \quad (126)$$

with

$$B_{\pm} = -\frac{11}{2N} \pm \frac{11}{2}, \quad (127)$$

leading to the evolution

$$C_{\pm}^{NLO}(\mu; \mu_0) = \left( 1 + \frac{\alpha_s(\mu)}{4\pi} J_{\pm} \right) \left( \frac{\alpha_s(\mu_0)}{\alpha_s(\mu)} \right)^{d_{\pm}} \left( 1 - \frac{\alpha_s(\mu_0)}{4\pi} [J_{\pm} - B_{\pm}] \right), \quad (128)$$

$$C_m^{NLO}(\mu; \mu_0) = \left( 1 + \frac{\alpha_s(\mu)}{4\pi} J_m \right) \left( \frac{\alpha_s(\mu_0)}{\alpha_s(\mu)} \right)^{d_m} \left( 1 - \frac{\alpha_s(\mu_0)}{4\pi} J_m \right). \quad (129)$$

We have

$$d_m = 4/\beta_0 \quad d_+ = 2/\beta_0 \quad d_- = -4/\beta_0. \quad (130)$$

The same equations can be written for  $O_i^{VRR}$  which will be useful for the discussion of the LR models, with identical results for the anomalous dimensions.

One may also consider the running of the  $|\Delta S| = 1$  local operators VLR. In the basis  $O_1^{VLR}, O_2^{VLR}$ , the anomalous dimensions are

$$\hat{\gamma}_{VLR}^{(0)} = \begin{bmatrix} 6/N & -6 \\ 0 & -6N + 6/N \end{bmatrix}, \quad (131)$$

$$\hat{\gamma}_{VLR}^{(1)} = \begin{bmatrix} 137/6 + 15/(2N^2) - 22/(3N)f & -100N/3 + 3/N + 22/3f \\ -71/2 \times N - 18/N + 4f & -203/6 \times N^2 + 479/6 + 15/(2N^2) + 10/3Nf - 22/(3N) \times f \end{bmatrix},$$

Introducing

$$\hat{V} = \begin{pmatrix} 3/2 & 0 \\ -1/2 & -1/2 \end{pmatrix}, \quad (132)$$

$$\hat{\gamma}_D^{(0)} = \hat{V}^{-1} \hat{\gamma}_{VLR}^{(0)T} \hat{V} = \begin{pmatrix} 6/N & 0 \\ 0 & -6N + 6/N \end{pmatrix}, \quad \gamma_1^{(0)} = 2, \quad \gamma_2^{(0)} = -16, \quad (133)$$

$$\hat{G} = \hat{V}^{-1} \hat{\gamma}_{VLR}^{(1)T} \hat{V}, \quad (134)$$

$$\hat{H}_{ij} = \delta_{ij} \gamma_i^{(0)} \frac{\beta_1}{2\beta_0^2} - \frac{\hat{G}_{ij}}{2\beta_0 + \gamma_i^{(0)} - \gamma_j^{(0)}} \quad (2\beta_0 + \gamma_i^{(0)} - \gamma_j^{(0)} \neq 0), \quad (135)$$

$$\hat{J} = \hat{V} \hat{H} \hat{V}^{-1}, \quad (136)$$

one can write down the evolution

$$\vec{C}^{LR}(\mu; \mu_0) = \left( 1 + \frac{\alpha_s(\mu)}{4\pi} \hat{J} \right) \hat{V} D(\mu; \mu_0) \hat{V}^{-1} \left( 1 - \frac{\alpha_s(\mu_0)}{4\pi} \hat{J} \right) \vec{C}^{LR}(\mu_0), \quad (137)$$

$$D(\mu; \mu_0) = \begin{pmatrix} (\alpha_s(\mu_0)/\alpha_s(\mu))^{d_1} & 0 \\ 0 & (\alpha_s(\mu_0)/\alpha_s(\mu))^{d_2} \end{pmatrix}, \quad (138)$$

with  $d_i = \gamma_i^{(0)}/(2\beta_0)$ .

## B.2 $|\Delta S| = 2$ operators

For  $|\Delta S| = 2$  operators, we recall the anomalous dimensions associated with the operator  $Q_V$

$$Q_V = (\bar{s}^\alpha \gamma_\mu P_L d^\alpha)(\bar{s}^\beta \gamma^\mu P_L d^\beta), \quad (139)$$

with

$$\gamma_V^{(0)} = 6 - 6/N, \quad (140)$$

$$\gamma_V^{(1)} = -19/6N - 22/3 + 39/N - 57/(2N^2) + 2/3f - 2/(3N)f, \quad (141)$$

$$J_V = \frac{d_V \beta_1}{\beta_0} - \frac{\gamma_V^{(1)}}{2\beta_0}, \quad d_V = \frac{\gamma_V^{(0)}}{2\beta_0}, \quad (142)$$

and we can write down a similar evolution for the  $|\Delta S| = 2$  local operators  $Q_1^{LR}, Q_2^{LR}$

$$Q_1^{LR} = (\bar{s}^\alpha \gamma_\mu P_L d^\alpha)(\bar{s}^\beta \gamma_\mu P_R d^\beta), \quad Q_2^{LR} = (\bar{s}^\alpha P_L d^\alpha)(\bar{s}^\beta P_R d^\beta), \quad (143)$$

with the anomalous dimensions

$$\begin{aligned} \hat{\gamma}_{LR}^{(0)} &= \begin{bmatrix} 6/N & 12 \\ 0 & -6N + 6/N \end{bmatrix}, \\ \hat{\gamma}_{LR}^{(1)} &= \begin{bmatrix} 137/6 + 15/(2N^2) - 22/(3N)f & 200N/3 - 6/N - 44/3f \\ 71/4 \times N + 9/N - 2f & -203/6 \times N^2 + 479/6 + 15/(2N^2) + 10/3Nf - 22/(3N) \times f \end{bmatrix}, \end{aligned} \quad (144)$$

Introducing

$$\hat{W} = \begin{pmatrix} 3/2 & 0 \\ 1 & 1 \end{pmatrix}, \quad (145)$$

$$\hat{\gamma}_D^{(0)} = \hat{W}^{-1} \hat{\gamma}_{LR}^{(0)T} \hat{W} = \begin{pmatrix} 6/N & 0 \\ 0 & -6N + 6/N \end{pmatrix} \quad \gamma_1^{(0)} = 2 \quad \gamma_2^{(0)} = -16, \quad (146)$$

$$\hat{G} = \hat{W}^{-1} \hat{\gamma}_{LR}^{(1)T} \hat{W}, \quad (147)$$

$$\hat{H}_{ij} = \delta_{ij} \gamma_i^{(0)} \frac{\beta_1}{2\beta_0^2} - \frac{\hat{G}_{ij}}{2\beta_0 + \gamma_i^{(0)} - \gamma_j^{(0)}} \quad (2\beta_0 + \gamma_i^{(0)} - \gamma_j^{(0)} \neq 0), \quad (148)$$

$$\hat{K} = \hat{W} \hat{H} \hat{W}^{-1}, \quad (149)$$

one can write down the evolution

$$\vec{C}^{LR}(\mu; \mu_0) = \left(1 + \frac{\alpha_s(\mu)}{4\pi} \hat{K}\right) \hat{W} D(\mu; \mu_0) \hat{W}^{-1} \left(1 - \frac{\alpha_s(\mu_0)}{4\pi} \hat{K}\right) \vec{C}^{LR}(\mu_0), \quad (150)$$

$$D(\mu; \mu_0) = \begin{pmatrix} (\alpha_s(\mu_0)/\alpha_s(\mu))^{d_1} & 0 \\ 0 & (\alpha_s(\mu_0)/\alpha_s(\mu))^{d_2} \end{pmatrix}, \quad (151)$$

with  $d_i = \gamma_i^{(0)} / (2\beta_0)$ . The associated LO anomalous dimensions are

$$\gamma_1^{(0)} = 2, \quad \gamma_2^{(0)} = -16, \quad (152)$$

and we have

$$d_1 = 1/\beta_0, \quad d_2 = -8/\beta_0, \quad d_V = 2/\beta_0. \quad (153)$$

## C LR case at NLO with the method of regions

### C.1 Contributions with $\log \beta$

If we consider the box with the Goldstone boson associated to  $W$  together with  $W'$ , the masses stem from the Goldstone boson coupling (evaluated at the scale  $\mu_W$ ), whereas the largest contribution to  $I_2$  comes from the range between  $\mu_W$  and  $\mu_R$ . We obtain

$$\begin{aligned} \xi_{a,UV}^{(W'2)} = & \sum_{r=\pm,i,j=1,2} \left( \frac{\alpha_s(\mu_W)}{\alpha_s(\mu_h)} \right)^{-d_r+d_i+2d_m} \left( \frac{\alpha_s(m_U)}{\alpha_s(\mu_h)} \right)^{-d_m} \left( \frac{\alpha_s(m_V)}{\alpha_s(\mu_h)} \right)^{-d_m} \left( \frac{\alpha_s(\mu_R)}{\alpha_s(\mu_h)} \right)^{d_r} \\ & \times \left[ \left( 1 + \frac{\alpha_s(\mu_h)}{4\pi} \hat{K} \right) \hat{W} \right]_{ai} \\ & \times R^{NLO} \left( -d_r + d_i - d_j, \right. \\ & \quad \left[ \hat{W}^{-1} \hat{a}_r^{(W'2)} \hat{V} \right]_{ij} [\hat{V}^{-1} \vec{C}_0]_j \\ & \quad \times \left( 1 - \frac{\alpha_s(\mu_R)}{4\pi} [J_r - B_r] - \frac{\alpha_s(\mu_W)}{4\pi} 2J_m + \frac{\alpha_s(m_U) + \alpha_s(m_V)}{4\pi} J_m \right) \\ & \quad - \frac{\alpha_s(\mu_W)}{4\pi} \left[ \hat{W}^{-1} \hat{a}_r^{(W'2)} \hat{V} \right]_{ij} [\hat{V}^{-1} \hat{J} \vec{C}_0]_j, \\ & \quad \left[ \hat{W}^{-1} [\hat{a}_r^{(W'2)} \hat{J} - \hat{K} \hat{a}_r^{(W'2)}] \hat{V} \right]_{ij} [\hat{V}^{-1} \vec{C}_0]_j + \left[ \hat{W}^{-1} \hat{a}_r^{(W'2)} \hat{V} \right]_{ij} [\hat{V}^{-1} \vec{C}_0]_j J_r, \\ & \quad \left. \mu_W, \mu_R \right), \end{aligned} \quad (154)$$

with the initial conditions for the evolution of the operators  $O_{1,2}^{VLR}$  and the coefficients for the matching from the two-point function of  $O_{\pm}^{VRR}$  and  $O_{1,2}^{VLR}$  to the local operators  $Q_{1,2}^{LR}$  at  $\mu = k^2$ .

$$\vec{C}_0 = \begin{pmatrix} 0 \\ -1/2 \end{pmatrix}, \quad C_a^{LR} \leftrightarrow \sum_{r,i} (\hat{a}_r^{(W'2)})_{ai} C_i^{VLR} C_r^{VRR}, \quad \hat{a}_r^{(W'2)} = \begin{pmatrix} (3r+1)/2 & r/2 \\ 0 & -1 \end{pmatrix}. \quad (155)$$

If we consider the box with  $W$  and a charged Higgs boson  $H$ , the masses stem from the Higgs couplings (to be evaluated at a high scale  $\mu_H$ ), whereas the largest contribution to  $I_2$  comes from the range between  $\mu_W$  and  $M_H$ . We obtain

$$\begin{aligned} \xi_{a,UV}^{(H2)} = & \sum_{l=\pm,i,j=1,2} \left( \frac{\alpha_s(\mu_W)}{\alpha_s(\mu_h)} \right)^{d_i-d_j} \left( \frac{\alpha_s(m_U)}{\alpha_s(\mu_h)} \right)^{-d_m} \left( \frac{\alpha_s(m_V)}{\alpha_s(\mu_h)} \right)^{-d_m} \left( \frac{\alpha_s(\mu_H)}{\alpha_s(\mu_h)} \right)^{d_j+2d_m} \\ & \times \left[ \left( 1 + \frac{\alpha_s(\mu_h)}{4\pi} \hat{K} \right) \hat{W} \right]_{ai} \\ & \times R^{NLO} \left( -d_l + d_i - d_j, \right. \\ & \quad \left[ \hat{W}^{-1} \hat{a}_l^{(H2)} \hat{V} \right]_{ij} [\hat{V}^{-1} \vec{C}_0]_j \\ & \quad \times \left( 1 - \frac{\alpha_s(\mu_W)}{4\pi} [J_l - B_l] - \frac{\alpha_s(\mu_H)}{4\pi} 2J_m + \frac{\alpha_s(m_U) + \alpha_s(m_V)}{4\pi} J_m \right), \\ & \quad \left[ \hat{W}^{-1} [\hat{a}_l^{(H2)} \hat{J} - \hat{K} \hat{a}_l^{(H2)}] \hat{V} \right]_{ij} [\hat{V}^{-1} \vec{C}_0]_j - \left[ \hat{W}^{-1} \hat{a}_l^{(H2)} \hat{V} \right]_{ij} [\hat{V}^{-1} \hat{J} \vec{C}_0]_j \\ & \quad \left. + \left[ \hat{W}^{-1} \hat{a}_l^{(H2)} \hat{V} \right]_{ij} [\hat{V}^{-1} \vec{C}_0]_j J_l, \mu_W, \mu_H \right), \end{aligned}$$

with the same initial conditions for the evolution of the operators  $Q_{1,2}^{VLL}$  and the coefficients for the matching from the two-point function of  $O_{\pm}^{VLL}$  and  $O_{1,2}^{VRL}$  to the local operators  $Q_{1,2}^{LR}$  at  $\mu = k^2$ .

$$C_a^{LR} \leftrightarrow \sum_{l,j} (\hat{a}_l^{(H2)})_{ai} C_j^{VRL} C_l^{VLL}, \quad \hat{a}_l^{(H2)} = \hat{a}_{r=l}^{(W'2)}. \quad (156)$$

One can check that the expressions from Ref. [39] are recovered at leading order.

If we consider  $\log \beta$  as small, we see that the diagrams are dominated by the region  $k^2 = \mathcal{O}(m_t^2, \mu_W^2)$  in all cases: this is obvious for  $tt$  and  $ct$  boxes, whereas the  $cc$  box receives only suppressed contributions from the region  $k^2 = \mathcal{O}(m_c^2)$ . We obtain thus expressions involving the averaging weight for constant terms  $R_1^{NLO}$

$$\bar{\eta}_{a,UV}^{(W'2)} = \xi_{a,UV}^{(W'2)}[R_1^{NLO}], \quad \bar{\eta}_{a,UV}^{(H2)} = \xi_{a,UV}^{(H2)}[R_1^{NLO}]. \quad (157)$$

In the case of a large  $\log \beta$ , we want to perform the resummation of the large  $\log \beta$  with  $R_{\log}^{NLO}$  and consider the rest of the contribution as dominated by the region  $k^2 = \mathcal{O}(m_t^2, \mu_W^2)$ . In the case of  $(W'2)$  we obtain

$$\begin{aligned} \bar{\eta}_{a,UV}^{(W'2)} = & \left[ F_{UV}^{(W'2)} \times \sum_{r=\pm, i,j=1,2} \left( \frac{\alpha_s(\mu_W)}{\alpha_s(\mu_h)} \right)^{-d_r+d_i+2d_m} \left( \frac{\alpha_s(m_U)}{\alpha_s(\mu_h)} \right)^{-d_m} \left( \frac{\alpha_s(m_V)}{\alpha_s(\mu_h)} \right)^{-d_m} \left( \frac{\alpha_s(\mu_R)}{\alpha_s(\mu_h)} \right)^{d_r} \right. \\ & \left. \times \hat{W}_{ai} \left[ \hat{W}^{-1} \hat{a}_r^{(W'2)} \hat{V} \right]_{ij} [\hat{V}^{-1} \vec{C}_0]_j + \log(\beta) \times \xi_{a,UV}^{(W'2)}[R_{\log}^{NLO}] \right] \frac{1}{\log(\beta) + F_{UV}^{(W'2)}} \end{aligned} \quad (158)$$

with the contributions from the constant term

$$F_{tt}^{(W'2)} = \frac{x_t^2 - 2x_t}{(x_t - 1)^2} \log(x_t) + \frac{x_t}{x_t - 1}, \quad F_{ct}^{(W'2)} = \frac{x_t}{x_t - 1} \log(x_t), \quad F_{cc}^{(W'2)} = 0, \quad (159)$$

and similarly for  $(H2)$

$$\begin{aligned} \bar{\eta}_{a,UV}^{(H2)} = & \left[ F_{UV}^{(H2)} \times \sum_{l=\pm, i,j=1,2} \left( \frac{\alpha_s(\mu_W)}{\alpha_s(\mu_h)} \right)^{d_i-d_j} \left( \frac{\alpha_s(m_U)}{\alpha_s(\mu_h)} \right)^{-d_m} \left( \frac{\alpha_s(m_V)}{\alpha_s(\mu_h)} \right)^{-d_m} \left( \frac{\alpha_s(\mu_H)}{\alpha_s(\mu_h)} \right)^{d_j+2d_m} \right. \\ & \left. \times \hat{W}_{ai} \left[ \hat{W}^{-1} \hat{a}_l^{(H2)} \hat{V} \right]_{ij} [\hat{V}^{-1} \vec{C}_0]_j + \log(\beta\omega) \times \xi_{a,UV}^{(H2)}[R_{\log}^{NLO}] \right] \frac{1}{\log(\beta\omega) + F_{UV}^{(H2)}} \end{aligned} \quad (160)$$

with the contributions from the constant term

$$F_{tt}^{(H2)} = x_t \frac{x_t + (x_t - 2) \log(x_t) - 1}{(x_t - 1)^2}, \quad F_{ct}^{(H2)} = \frac{x_t}{x_t - 1} \log(x_t), \quad F_{cc}^{(H2)} = 0. \quad (161)$$

## C.2 Contributions without $\log \beta$

If we consider the box with the Goldstone associated with  $W$  and a charged Higgs boson  $H$ , the masses stem from the Higgs couplings, the Goldstone boson couplings and the propagator, whereas

the largest contribution to  $I_1$  comes from the range between  $m_V$  and  $\mu_W$ . We obtain

$$\begin{aligned} \bar{\eta}_{a,UV}^{(H1)} = & \sum_{b,i,j,j',k,k'=1,2} \left( \frac{\alpha_s(m_U)}{\alpha_s(\mu_h)} \right)^{-3d_m} \left( \frac{\alpha_s(m_V)}{\alpha_s(\mu_h)} \right)^{d_i-d_k-d_{k'}-d_m} \left( \frac{\alpha_s(\mu_W)}{\alpha_s(\mu_h)} \right)^{d_k+2d_m} \left( \frac{\alpha_s(\mu_H)}{\alpha_s(\mu_h)} \right)^{d_{k'}+2d_m} \\ & \times \bar{a}_{b,j,j'}^{(H1)} \left[ \left( 1 + \frac{\alpha_s(\mu_h)}{4\pi} \hat{K} \right) \hat{W} \right]_{ai} \left[ \hat{V}^{-1} \left( 1 - \frac{\alpha_s(\mu_W)}{4\pi} \hat{J} \right) \vec{C}_0 \right]_k \left[ \hat{V}^{-1} \left( 1 - \frac{\alpha_s(\mu_H)}{4\pi} \hat{J} \right) \vec{C}_0 \right]_{k'} \\ & \times R^{NLO} \left( d_i - d_k - d_{k'} + 2d_m, \right. \\ & \quad \left. \hat{W}_{ib}^{-1} \hat{V}_{jk} \hat{V}_{j'k'} \times \left( 1 - \frac{\alpha_s(\mu_W)}{4\pi} 2J_m - \frac{\alpha_s(\mu_H)}{4\pi} 2J_m + \frac{\alpha_s(m_U) + \alpha_s(m_V)}{4\pi} 3J_m \right), \right. \\ & \quad \left. - 2J_m \hat{W}_{ib}^{-1} \hat{V}_{jk} \hat{V}_{j'k'} - (\hat{W}^{-1} \hat{K})_{ib} \hat{V}_{jk} \hat{V}_{j'k'} + \hat{W}_{ib}^{-1} (\hat{J} \hat{V})_{jk} \hat{V}_{j'k'} + \hat{W}_{ib}^{-1} \hat{V}_{jk} (\hat{J} \hat{V})_{j'k'}, \right. \\ & \quad \left. m_V, \mu_W \right), \end{aligned} \quad (162)$$

where  $\bar{a}_{a,ij}^{(H1)}$  provides the coefficients for the matching from the two-point function of  $O_{1,2}^{VLR}$  to the local operators  $Q_{1,2}^{LR}$  at  $\mu = k^2$ :

$$C_a^{LR} \leftrightarrow \sum_{ij} \bar{a}_{a,ij}^{(H1)} C_i^{VLR} C_j^{VRL}, \quad (163)$$

with the non-vanishing entries

$$\bar{a}_{1,12}^{(H1)} = -2, \quad \bar{a}_{1,21}^{(H1)} = -2, \quad \bar{a}_{1,11}^{(H1)} = -6, \quad \bar{a}_{2,22}^{(H1)} = 4. \quad (164)$$

The only relevant case is  $tt$ , where  $R^{NLO}$  can be replaced by  $R_1^{NLO}$ .

If we consider tree-level  $H^0$  exchanges, we have

$$\begin{aligned} \bar{\eta}_{a,UV}^{(H)} = & \left( \frac{\alpha_s(m_U)}{\alpha_s(\mu_h)} \right)^{-d_m} \left( \frac{\alpha_s(m_V)}{\alpha_s(\mu_h)} \right)^{-d_m} \left( \frac{\alpha_s(\mu_H)}{\alpha_s(\mu_h)} \right)^{2d_m} \\ & \times \left( 1 - \frac{\alpha_s(\mu_H)}{4\pi} 2J_m + \frac{\alpha_s(m_U) + \alpha_s(m_V)}{4\pi} J_m \right) \\ & \times \left[ \left( 1 + \frac{\alpha_s(\mu_h)}{4\pi} \hat{K} \right) \hat{W} \left( \frac{\alpha_s(\mu_H)}{\alpha_s(\mu_h)} \right)^{\vec{d}} \hat{W}^{-1} \left( 1 - \frac{\alpha_s(\mu_H)}{4\pi} \hat{K} \right) \vec{C}_0 \right]_a, \end{aligned} \quad (165)$$

where the matching yields the value of the Wilson coefficients for the  $|\Delta S| = 2$  operators at the high scale. One can check that the expressions from Ref. [39] are recovered at leading order.

## D Result for the individual diagrams

In order to evaluate the diagrams necessary to determine the short-distance QCD corrections for meson mixing in Left-Right models we used the packages Feyncalc and TARCER [53]. We only discuss the finite parts of the diagrams here, the infinite parts being discussed in Tab. 4 and Eqs. (92)-(93).

### D.1 Diagrams $D_i$

The two-loop diagrams in Fig. 4 have the following structure

$$\begin{aligned} D_i^{rl} = & -i \frac{m_c^2}{64\pi^2} \frac{\alpha_s}{4\pi} \left( \left[ -\frac{1}{\epsilon} \left( C_i^{rl} d_i - 2 \widetilde{C}_i^{rl} \tilde{d}_i \right) + (C_i^{rl} A_i - 2 \widetilde{C}_i^{rl} B_i) \right] P_R \otimes P_L \right. \\ & \left. + (B_i C_i^{rl} - \widetilde{C}_i^{rl} A_i/2) \gamma_\mu P_R \otimes \gamma_\mu P_L \dots \right) \end{aligned} \quad (166)$$

	$D_0$	$D_1$	$D_2$	$D_3$
$C^{rl}$	1	$\frac{N^2-1}{2N} - \tau_{rl}$	$-\frac{1}{2N}$	$-\frac{1}{2N} - \tau_{rl}$
$\tilde{C}^{rl}$	$-2\tau_{rl}$	$\frac{\tau_{rl}}{N}$	$\frac{1}{2} - \frac{N^2-1}{N}\tau_{rl}$	$\frac{1}{2} + \frac{1}{N}\tau_{rl}$
	$D_4$	$D_5$	$D_6$	$D_7$
$C^{rl}$	$-\frac{1}{2N}$	$\frac{N^2-1}{2N}$	$\frac{N^2+rN-1}{2N}$	$\frac{rN-1}{2N}$
$\tilde{C}^{rl}$	$\frac{1}{2} - \frac{N^2-1}{N}\tau_{rl}$	$-\frac{(N^2-1)}{N}\tau_{rl}$	$\frac{(N^2-1)l-r}{2N}$	$\frac{l(N^2-1)+N-r}{2N}$

Table 5: Colour factors for the diagrams  $D_i$ .  $r, l$  can have the values  $\pm 1$  and  $\tau_{rl}$  is defined in Eq. (42)

where the ellipsis stands for possible other operators uninteresting for our purpose.  $C_i^{rl}$  and  $\tilde{C}_i^{rl}$  are colour factors given in Tab. 5. This provides also the notation in Tab. 4, as we have written the divergent part proportional to the operator  $P_R \otimes P_L$  explicitly (a similar divergent part is also present for the other operator). The diagram  $D_8 = 0$  for zero external momenta. Other classes can be obtained through either a rotation of 90 or 180 degrees, or a left-right reflection (resulting in the exchange  $r \leftrightarrow l$  in the colour factors in some cases, see Tab. 5).

The finite gauge-independent part is given by

$$\begin{aligned}
A_1 &= 6(-2(R-2)\log(m_c^2/\mu^2) + \log^2(m_c^2/\mu^2) + 2R/3 - R_2 - \pi^2/6 + 8/3) , \\
A_2 &= -6(\log(m_c^2/\mu^2) + R + 1/2) , \\
A_3 &= \frac{3}{2}(12\log(m_s^2/\mu^2) - 13) , \\
B_3 &= -3(\log(m_s^2/\mu^2) + \log(m_c^2/\mu^2) + 7/6) , \\
A_4 &= 12\log(m_c^2/\mu^2) + 59 , \\
A_5 &= -2(3\log^2(m_c^2/\mu^2) + 4\log(m_c^2/\mu^2) + 3) , \\
A_6 &= -6(\log(m_c^2/\mu^2) + 7/12) , \\
A_7 &= 6\log^2(m_c^2/\mu^2) - 16\log(m_c^2/\mu^2) + 5 , \\
\end{aligned} \tag{167}$$

while the gauge-dependent part

$$\begin{aligned}
A_1^\xi &= 2(-2(R-2)\log(m_c^2/\mu^2) + \log^2(m_c^2/\mu^2) - 2R - R_2 + 7 - \pi^2/6) , \\
A_2^\xi &= -4((R-1)\log(m_c^2/\mu^2) + R + R_2/2 - 1 + \pi^2/12) , \\
A_3^\xi &= 2(\log(m_s^2/\mu^2)^2 + 2(\log(m_s^2/\mu^2) - 1)\log(m_c^2/\mu^2) + 4\log(m_s^2/\mu^2) - \log^2(m_c^2/\mu^2) + \pi^2/6 - 5) , \\
B_3^\xi &= -\log(m_s^2/\mu^2) - \log(m_c^2/\mu^2) - 1/2 , \\
A_4^\xi &= -4(\log^2(m_c^2/\mu^2) + 2\log(m_c^2/\mu^2) + 5) , \\
A_5^\xi &= 2(\log^2(m_c^2/\mu^2) + 2\log(m_c^2/\mu^2) + 5) , \\
A_6^\xi &= -2(\log^2(m_c^2/\mu^2) + 2\log(m_c^2/\mu^2) + 5) , \\
A_7^\xi &= 2(\log^2(m_c^2/\mu^2) + 2\log(m_c^2/\mu^2) + 5) . \\
\end{aligned} \tag{168}$$

$R$  and  $R_2$  are defined as

$$\begin{aligned}
R &= \frac{1}{m_s^2 - m_d^2}(m_s^2 \log(m_s^2/\mu^2) - m_d^2 \log(m_d^2/\mu^2)) , \\
R_2 &= \frac{1}{m_s^2 - m_d^2}(m_s^2 \log^2(m_s^2/\mu^2) - m_d^2 \log^2(m_d^2/\mu^2)) . \\
\end{aligned} \tag{169}$$

$L_k$	$L_1$	$L_2$	$L_3$
$C^k$	$\frac{N^2-1}{2N}$	$-\frac{1}{2N}$	$-\frac{1}{2N}$
$\tilde{C}^k$	0	$\frac{1}{2}$	$\frac{1}{2}$

Table 6: Colour factors for the diagrams  $L_k$ .

## D.2 Diagrams $L_i$

The diagrams in Fig. 5 with insertions from the operators  $Q_i$  divided by  $\epsilon$  yield

$$Q_{ii}^{(1)} = \sum_{k=1}^3 (\bar{A}_{ii}^k C_k + f_i \bar{A}_{ji}^k \tilde{C}_k) Q_i, \quad Q_{ij}^{(1)} = \sum_{k=1}^3 (\bar{A}_{ii}^k \tilde{C}_k / f_i + \bar{A}_{ji}^k C_k) Q_j, \quad Q_i^{(1)} = Q_{ii}^{(1)} + Q_{ij}^{(1)} = \sum_m b_{mi} Q_m, \quad (170)$$

where  $k$  denotes the diagram  $k$  and  $j = 2, 1$ .  $C_k$  and  $\tilde{C}_k$  are the colour factors given in Tab. 6 and  $f_i$  are coefficients coming from the Fierz transformation,  $f_1 = -1/2$  and  $f_2 = -2$ . The  $2 \times 2$  matrices  $\bar{A}^{1,2}$  turn out to be diagonal.

These diagrams have a finite and an infinite parts. The former reads:

$$\bar{A}^1 = \begin{pmatrix} \frac{3}{2}R - \frac{5}{4} + G_a \xi & 0 \\ 0 & G^{\text{ind}} + G_a \xi \end{pmatrix}, \quad (171)$$

$$\bar{A}^2 = \begin{pmatrix} G^{\text{ind}} + G_a \xi & 0 \\ 0 & \frac{3}{2}R - \frac{9}{4} + G_a \xi \end{pmatrix}. \quad (172)$$

and

$$\bar{A}^3 = \begin{pmatrix} \frac{3}{2} \left( \log \left( \frac{m_s^2}{\mu^2} \right) - \frac{1}{2} \right) + G_b \xi & \frac{1}{4} \left( 3 \log \left( m_s^2 / \mu^2 \right) - \frac{5}{2} \right) + \frac{1}{4} \xi \left[ \log \left( m_s^2 / \mu^2 \right) - \frac{3}{2} \right] \\ 3 \log \left( m_s^2 / \mu^2 \right) - \frac{11}{2} + \xi \left[ \log \left( m_s^2 / \mu^2 \right) - \frac{5}{2} \right] & \frac{3}{2} \left( \log \left( \frac{m_s^2}{\mu^2} \right) - \frac{1}{2} \right) + G_b \xi \end{pmatrix} \quad (173)$$

with

$$\begin{aligned} G^{\text{ind}} &= \frac{1}{2} \left( -2R + 3R_2 + \frac{\pi^2}{2} + 2 \right), \\ G_a &= \frac{1}{4} \left( -4R + 2R_2 + \frac{\pi^2}{3} + 4 \right), \\ G_b &= -\frac{1}{2} \left( \log^2 \left( \frac{m_s^2}{\mu^2} \right) + \frac{\pi^2}{6} \right). \end{aligned} \quad (174)$$

Note that the graph  $L_2$  can be obtained from  $L_1$  by a Fierz transformation. It is easy to check that this implies that  $\bar{A}_1$  and  $\bar{A}_2$  are obtained from one another by interchanging their diagonal elements. One can see that this is indeed the case for the gauge-dependent terms but not for the terms independent of the regularisation in the gauge-independent ones. This comes from the fact that the relations for the Fierz transformation are generally valid only in 4 dimensions. The corrections in  $D$  dimensions define the evanescent operators  $E_5$  and  $E_6$ , Eq. (55).

## References

- [1] J. C. Pati and A. Salam, Phys. Rev. D **10** (1974) 275 [Phys. Rev. D **11** (1975) 703].
- [2] R. N. Mohapatra and J. C. Pati, Phys. Rev. D **11** (1975) 566.

- [3] R. N. Mohapatra and J. C. Pati, Phys. Rev. D **11** (1975) 2558.
- [4] G. Senjanovic and R. N. Mohapatra, Phys. Rev. D **12** (1975) 1502.
- [5] G. Senjanovic, Nucl. Phys. B **153** (1979) 334.
- [6] D. Chang, Nucl. Phys. B **214** (1983) 435.
- [7] Y. Zhang, H. An, X. Ji and R. N. Mohapatra, Nucl. Phys. B **802** (2008) 247 [arXiv:0712.4218 [hep-ph]].
- [8] A. Maiezza, M. Nemevsek, F. Nesti and G. Senjanovic, Phys. Rev. D **82** (2010) 055022 [arXiv:1005.5160 [hep-ph]].
- [9] D. Guadagnoli and R. N. Mohapatra, Phys. Lett. B **694** (2011) 386 [arXiv:1008.1074 [hep-ph]].
- [10] R. N. Mohapatra and G. Senjanovic, Phys. Rev. D **23** (1981) 165.
- [11] N. G. Deshpande, J. F. Gunion, B. Kayser and F. I. Olness, Phys. Rev. D **44** (1991) 837.
- [12] S. Descotes-Genon, J. Matias and J. Virto, Phys. Rev. D **88** (2013) 074002 [arXiv:1307.5683 [hep-ph]].
- [13] S. Descotes-Genon, L. Hofer, J. Matias and J. Virto, JHEP **1412** (2014) 125 [arXiv:1407.8526 [hep-ph]].
- [14] S. Descotes-Genon, L. Hofer, J. Matias and J. Virto, arXiv:1510.04239 [hep-ph].
- [15] K. Hsieh, K. Schmitz, J. H. Yu and C.-P. Yuan, Phys. Rev. D **82** (2010) 035011 [arXiv:1003.3482 [hep-ph]].
- [16] G. Aad *et al.* [ATLAS Collaboration], Eur. Phys. J. C **72** (2012) 2056 [arXiv:1203.5420 [hep-ex]].
- [17] V. Khachatryan *et al.* [CMS Collaboration], Eur. Phys. J. C **74** (2014) 11, 3149 [arXiv:1407.3683 [hep-ex]].
- [18] H. Harari and M. Leurer, Nucl. Phys. B **233** (1984) 221.
- [19] G. Beall, M. Bander and A. Soni, Phys. Rev. Lett. **48** (1982) 848.
- [20] P. Langacker and S. U. Sankar, Phys. Rev. D **40** (1989) 1569.
- [21] G. Barenboim, J. Bernabeu, J. Prades and M. Raidal, Phys. Rev. D **55** (1997) 4213 [hep-ph/9611347].
- [22] G. Barenboim, M. Gorbahn, U. Nierste and M. Raidal, Phys. Rev. D **65** (2002) 095003 [hep-ph/0107121].
- [23] R. N. Mohapatra, F. E. Paige and D. P. Sidhu, Phys. Rev. D **17** (1978) 2462.
- [24] R. N. Mohapatra, G. Senjanovic and M. D. Tran, Phys. Rev. D **28** (1983) 546.
- [25] G. Barenboim, J. Bernabeu and M. Raidal, Nucl. Phys. B **478** (1996) 527 [hep-ph/9608450].
- [26] M. Blanke, A. J. Buras, K. Gemmeler and T. Heidsieck, JHEP **1203** (2012) 024 [arXiv:1111.5014 [hep-ph]].
- [27] S. Bertolini, A. Maiezza and F. Nesti, Phys. Rev. D **89** (2014) 9, 095028 [arXiv:1403.7112 [hep-ph]].

[28] N. Carrasco *et al.* [ETM Collaboration], Phys. Rev. D **92** (2015) 3, 034516 [arXiv:1505.06639 [hep-lat]].

[29] G. Buchalla, A. J. Buras and M. E. Lautenbacher, Rev. Mod. Phys. **68**, 1125 (1996) [hep-ph/9512380].

[30] F. J. Gilman and M. B. Wise, Phys. Rev. D **27** (1983) 1128.

[31] A. J. Buras, M. Jamin and P. H. Weisz, Nucl. Phys. B **347**, 491 (1990).

[32] A. J. Buras, M. Jamin, M. E. Lautenbacher and P. H. Weisz, Nucl. Phys. B **370**, 69 (1992) [Nucl. Phys. B **375**, 501 (1992)].

[33] S. Herrlich and U. Nierste, Nucl. Phys. B **419**, 292 (1994) [hep-ph/9310311].

[34] S. Herrlich and U. Nierste, Nucl. Phys. B **455**, 39 (1995) [hep-ph/9412375].

[35] S. Herrlich and U. Nierste, Nucl. Phys. B **476**, 27 (1996) [hep-ph/9604330].

[36] A. J. Buras, M. Misiak and J. Urban, Nucl. Phys. B **586**, 397 (2000) [hep-ph/0005183].

[37] A. I. Vainshtein, V. I. Zakharov, V. A. Novikov and M. A. Shifman, Sov. J. Nucl. Phys. **23**, 540 (1977) [Yad. Fiz. **23**, 1024 (1976)]. Phys. Rev. D **16**, 223 (1977).

[38] M.I. Vysotskiĭ, Sov. J. Nucl. Phys. 31 (1980) 797.

[39] G. Ecker and W. Grimus, Nucl. Phys. B **258**, 328 (1985).

[40] I. I. Y. Bigi and J. M. Frère, Phys. Lett. B **129**, 469 (1983) [Phys. Lett. B **154**, 457 (1985)].

[41] J. Brod and M. Gorbahn, Phys. Rev. Lett. **108**, 121801 (2012) [arXiv:1108.2036 [hep-ph]].

[42] A.I. Vainstein and I.B. Khriplovich, Pis'ma Zh. Eksp. Teor. Fiz. 18 (1973) 141 [JETP Lett. 18 (1073) 63].

[43] M. K. Gaillard and B. W. Lee, Phys. Rev. D **10**, 897 (1974).

[44] J. Brod and M. Gorbahn, Phys. Rev. D **82**, 094026 (2010) [arXiv:1007.0684 [hep-ph]].

[45] D. Chang, J. Basecq, L. F. Li and P. B. Pal, Phys. Rev. D **30**, 1601 (1984).

[46] J. Basecq, L. F. Li and P. B. Pal, Phys. Rev. D **32**, 175 (1985).

[47] Z. Gagyi-Palffy, A. Pilaftsis and K. Schilcher, Nucl. Phys. B **513** (1998) 517 [hep-ph/9707517].

[48] W. S. Hou and A. Soni, Phys. Rev. D **32**, 163 (1985).

[49] V. Bernard, S. Descotes-Genon and L. Vale Silva, in preparation.

[50] M. Kenmoku, Y. Miyazaki and E. Takasugi, Phys. Rev. D **37** (1988) 812.

[51] A. J. Buras and P. H. Weisz, Nucl. Phys. B **333** (1990) 66.

[52] M. J. Dugan and B. Grinstein, Phys. Lett. B **256**, 239 (1991).

[53] R. Mertig and R. Scharf, Comput. Phys. Commun. **111**, 265 (1998) [hep-ph/9801383].